THE HONG KONG POLYTECHNIC UNIVERSITY

Department of Electrical Engineering

Development of Hybrid Constrained Genetic Algorithm and Particle Swarm Optimisation Algorithm for Load Flow

TING Tiew On

A thesis submitted in partial fulfilment of the requirements for the Degree of Doctor of Philosophy

Sept 2007

CERTIFICATE OF ORIGINALITY

I hereby declare that this thesis is my own work and that, to the best of my knowledge and belief, it reproduces no material previously published or written, nor material that has been accepted for the award of any other degree or diploma, except where due acknowledgement has been made in the text.

_____

TING Tiew On

Dedicated to my beloved family,

for their enormous love and encouragement.

Abstract

The calculation of active and reactive power flow in an electric network to ensure satisfactory voltage profile and loading of transmission circuits is of utmost importance in power system planning, operation and control. Conventional methods such as the Newton-Raphson and the fast decoupled load flow methods have been widely used by the power utilities. However, when a power system becomes highly stressed, it will be difficult for conventional methods to converge. Furthermore, as more and more non-linear devices, for instance Flexible AC transmission system (FACTS) devices, are used in power transmission networks, conventional load flow methods may have difficulties in solving the load flow problem and hence it is also difficult to use these methods to determine the maximum loading points and to assess the static voltage stability of a power system.

To overcome the above mentioned problems, this thesis is devoted to the development of alternative approach in dealing with the load flow problem based on evolutionary computation. In particular, this thesis reports work on the formation of a hybrid algorithm comprising of the constrained genetic algorithm and Particle Swarm Optimisation. Based on the virtual population concept embedded in a constrained genetic algorithm for load flow previously developed, the Particle Swarm Optimisation method is utilised as an efficient means to

generate high quality candidate solutions in the virtual population during the optimisation process in seeking for the load flow solution. An experimental approach is reported in the thesis on finding the best parameter settings for use in the Particle Swarm Optimisation part of the hybrid algorithm. The performance of the developed algorithm is demonstrated using the IEEE 30-, 57- and 118-bus systems. The results in finding the maximum loading points using the new hybrid method are presented and discussed. The use of the hybrid algorithm in determining the Type-1 load flow solutions for voltage stability assessment is also demonstrated and described in the thesis.

This thesis also develops a stochastic method for determining the maximum loading point of power system using the developed hybrid constrained genetic algorithm and Particle Swarm Optimisation and a strategy in starting the search for the maximum loading point in the infeasible operation region of the power system. The new approach is applied to IEEE 14-, 30- and 57-bus test systems and the results are presented.

The new hybrid algorithm developed in the thesis is found to be powerful in solving the load flow problem for heavy-loaded systems and is efficient in locating the Type-I load flow solutions and determining the maximum loading point of a power system.

Publications

Book Chapter

1. T.O. Ting, K.P. Wong, and C.Y. Chung, "A Hybrid Genetic Algorithm/Particle Swarm Approach for Evaluation of Power Flow in Electric Network," *Lecture Notes in Artificial Intelligence (LNAI)*, Vol 3930, pp. 908-917, May 2006.

Journal Papers

1. T.O. Ting, K.P. Wong, and C.Y. Chung, "A Hybrid Constrained Genetic Algorithm / Particle Swarm Optimisation Load Flow Algorithm" Accepted by *IET Generation, Transmission & Distribution,* June 2008.

Refereed Conference Papers

1. T.O. Ting, K.P. Wong, and C.Y. Chung, "Two-phase Particle Swarm Optimization for Load Flow Analysis," *Proc. 2006 International Conference on Systems, Man and Cybernetics (SMC 2006),* Taipei, Taiwan, 8-11 October 2006, Vol 1, pp. 2345–2350.

2. T.O. Ting, K.P. Wong, and C.Y. Chung, "Locating Type-1 Load Flow Solutions using Hybrid Evolutionary Algorithm," *Proc. of the 5th IEEE International Conference on Machine Learning and Cybernetics (ICMLC 2006),* Dalian, China, 13-16 August 2006, Vol 7, pp. 4093-4098. (Awarded 2006 IEEE SMC ICMLC Best Student Paper Award)

3. T.O. Ting, K.P. Wong, and C.Y. Chung, "Investigation of Hybrid Genetic Algorithm / Particle Swarm Optimization Approach for the Power Flow Problem," *Proc. of the 4th IEEE International Conference on Machine*

Learning and Cybernetics (ICMLC 2005), Guangzhou, China, 19-21 Aug 2005, Vol 1, pp. 436-440.

Acknowledgements

Many people have contributed to the success of this Ph.D thesis. It would never have been completed without the generous help and support that I received from numerous people along the way. It is my great pleasure to take this opportunity to extend my sincere appreciation to these wonderful people.

First and foremost, I am honoured to be awarded the prestigious international scholarship by The Hong Kong Polytechnic University. The award has given me a great motivation to exert in my PhD study so as to contribute to the portal knowledge of the university and the society.

I would like to express my utmost gratitude to my chief supervisor, Prof. K..P. Wong for his continuous guidance, patience, encouragement and support to complete this Ph.D. degree. Prof. Wong has been constantly emphasizing on high quality in all research works and has reminded me of its importance when doing research. Not only have I grasped the importance of quality research, I have also learned to do research in a methodological manner. His expert advice, professionalism and kindness are deeply rooted in my heart.

My sincere appreciation also goes to my co-supervisor, Dr. C. Y. Chung for providing me with the essential tools for doing my research. Despite his busy schedule, he has been very generous in sharing his knowledge and expertise and

in finding useful information which I need for my research and has assisted me in solving some of the tough problems I had encountered in my research.

I am also grateful to my parents for their love, encouragement, prayers, support and many sacrifices and also for instilling the importance of education since my childhood. They have shared their wisdom with me and given me invaluable moral support, care and advice in my study; as well as in my life.

Lastly, to all the members of Computational Intelligence Applications Research Laboratory (CIARLab), my sincere thanks to all of you for your generous support and kind assistant. It has been truly great to have you all by my side in this lifelong adventure of pursuing knowledge. Some names worth to be mentioned are Su Sheng, Wang Zhen, Dai Bo, Zhang Shengxiang and Wu Guoyue. My heartfelt thanks to you all!

Contents

List of Tables

List of Figures

Summary of Original Contributions

A summary of the original contributions made in this thesis is given below.

(a) Development of hybrid optimisation method which is based on Genetic Algorithm (GA) and Particle Swarm Optimisation (PSO) algorithms for load flow problem.

(b) Determination of parameter settings for hybrid CGA/PSO algorithm to solve the load flow problem effectively.

(c) Development of Fast Infeasible Method (FIM) for the calculation of Maximum Loading Point (MLP) of a power system.

Chapter 1

1. Introduction

1.1 Introduction

Network equations can be formulated systematically in a variety of forms. However, the node-voltage method, which is the most suitable form for many power system analyses, is commonly applied. The formulation of the network equations in the nodal admittance form results in complex linear simultaneous algebraic equations in terms of node currents. When node currents are specified, the set of linear equations can be solved for the node voltages. However, in power system, powers are known rather than currents. Thus, the resulting equations in terms of power, known as the power flow equation, become nonlinear and must be solved by iterative techniques. Power flow studies, commonly referred to as load flow, are the backbone of power system analysis and design. The load flow problem is of primary importance in determining the voltage levels and power flows within the power system. It is used in daily

system analysis, operation and future planning for expansion. In other words, load flow problem is the backbone of power system analysis and design. They are necessary for planning, operation, economic scheduling and exchange of power between utilities. In addition, load flow analysis is required in many other analyses such as transient stability and contingency studies. Some important areas of stability study involving the type of load flow solutions, maximum loading point (MLP) are covered in this chapter. In addition to this the contingency analyses involving branch and generator outages are also discussed. The layout of the complete thesis is carefully arranged in section 1.6.

1.2 Conventional Solution Techniques

A very concise discussion on conventional techniques has been given in [1]-[3]. Generally, the Newton Raphson (NR) method [4] and a variety of its modifications are most popular numeric approach for load flow problems. This technique has the advantage of being very fast to converge, usually within ten iterations. Other conventional methods are Decoupled methods [5]-[7] and Gauss-Seidel method [8]. Because of its quadratic convergence, Newton's method is mathematically superior to the Gauss-Seidel method and is less prone to divergence with ill-conditioned problems. For large power systems, the Newton Raphson method is found to be more efficient and practical.

It is widely known that the NR method has very good quadratic convergence if initial estimates are close to a solution point. However, if a

solution point is far or ill-conditioned one, convergence of the NR method can be slow or does not converge at all. To overcome this problem, a number of numeric techniques are proposed [9]. The general idea behind all of them is to apply corrections to each step of methods in such a way that iterative processes do no oscillate or diverge.

In [10], B. Borkowska developed the Probabilistic Load Flow (PLF), which is able to cope with uncertainty of node data. In PLF, the net loads are given as a set of values together with additional information on the frequency of its accuracy. These input parameters of the load flow problem are treated as random variables defined in terms of probability density functions (pdfs) and transformed into state and output random variables also defined in terms of pdfs. This approach has been analytically formulated in [10] and further developed and applied in various recent works [11, 12] .

Thorp et al. [13] pointed out that the regions of attraction of load flow solutions calculated by Newton-Raphson have complicated boundaries which are actually fractals. The complex nature of the load flow solution space is illustrated graphically by I. A. Hiskens in [15], showing a solution space of Q-P curve has a hole through it. Despite many advances in order to improve both the efficiency and robustness of the methods have been reported, some difficulties can still be observed in many practical situations.

1.3 Type-1 Load Flow Solutions

Due to its nonlinearity, the load flow problem can have a number of distinct solutions. Studies of the multiple solution load flow problem play an important role in determining of stability margins and proximity to a voltage collapse [16, 17]. Thus, it is important for an effective algorithm to locate all multiple load flow solutions accurately with low computational requirements [18, 19]. In order to obtain multiple load flow solutions, Tamura et al have used a set of quadratic equations and the NR optimal multiplier method [22]. Iba et al used the Tamura's approach and some newly discovered convergence peculiarities of the NR method with optimal multipliers to find a pair of closest multiple solutions if there is one [25]. The pair of multiple power flow solutions is also calculated by H. Mori in [21] using mathematical programming.

It is observed from experimental results in [25] that if a point comes close to a line connecting a couple of distinct solutions, a further NR iterative process in rectangular form goes along this line. Another observation in [25] is that in vicinity of a bifurcation point the NR method with the optimal multiplier gives a trajectory which tends to the straight line connecting a pair of closely located but distinct solutions. These features are effectively used in [25] to locate multiple load flow solutions.

The studies in [17] show that the voltage collapse phenomena is associated with the multiple load flow solutions present due to the nonlinearity of the load

flow equations. The maximum number of solution exists in a system is 2^n where n is the number of buses excluding the slack bus [22]. Thus there exists a demand for a methodology which has the capability of classifying the nature of multiple solutions as well as for finding them numerically.

In [23], a special probability-one homotopy method is tailored to find all the load-flow equation of 5-bus and 7-bus systems. However, this method demands the need of tracing a certain number of homotopy curves. The solution is further verified in [18] with reduction in time requirement. However, it is still impractical for moderately sized power system due to the computational burden. Although the work in [14, 23, 24] is able to locate all the load flow solutions, the connection of these solutions in regards to voltage stability remains to be indistinct.

Type-1 solution simply means that the corresponding Jacobian matrix of the load flow solution set has exactly one eigenvalue with a positive real part and the rest of the eigenvalues have negative real parts. In general, a solution is considered Type-k when there are k positive values for the real part of the eigenvalues whereby these eigenvalues can be either complex number or real number. In other words, Type-1 solutions have only one eigenvalue with a positive real part while Type-2 solution has two positive real part values. Works presented in [26, 27] link the Type-1 solutions to the voltage stability assessment by stating that only Type-1 load flow solutions are closely associated

with voltage instability phenomenon. Based on this fact, the computational cost can be further reduced by locating only the Type-1 load flow solutions while the other solutions are not a major concern for stability assessment. Recently, works in [27, 28] present different strategies in locating Type-1 load flow solutions. However, the method in [27] lacks in the ability in locating all the possible Type-1 solutions present in a large system while the performance of CPFLOW-based algorithm in [28] is unknown for large system as only small systems are adopted for test problems.

As an operating point moves closer to the solution boundary, so to does a corresponding unstable low-voltage solution. The stability boundary is tied to this low-voltage solution. Therefore, as the two solution points merge, the stability boundary approaches the operating point, and the stability region shrinks [29]. It is interesting to note that the operating point involved in this situation is a Type-1 solution whereas the other solution is a normal solution.

1.4 Maximum Loading Point (MLP)

Over the previous decades numerous techniques have been developed to determine the loadability limits of power systems. The calculation of the Maximum Loading Point (MLP) is usually done when the system is operating normally and when contingency occurs. The following sub-sections discuss both of these.

1.4.1 MLP Determination during Stable State

Several classes of methods exist for determination of MLP when the system is operating normally. One class of methods utilises the distance between the operating load-flow solution and bifurcation point of a system [17, 22]. Yet another class of methods investigates the voltage stability limits based upon different types of load-flow analysis [23, 24], energy methods [30] and sensitivity analysis [31, 32]. Works in [33, 34] utilise the minimum singular value of the Jacobian matrix as a voltage stability index. The maximum loading point (MLP) is estimated in [35] by using a set of stable operating point which is based on the analysis of Jacobian matrix behaviour. Meanwhile, continuation methods are widely known as very powerful, though slow, methods to estimate the system maximum loading [36].

Apart from the above methods, load flow study still remains a very important approach in checking on the maximum loading point of a power system. Efficient and reliable load flow solutions, such as the Newton-Raphson (NR) [37] and the fast decoupled load flow [5], have been widely used by the power industry. However, when a power system becomes highly stressed, it will be difficult for conventional methods to converge. Also the employment of Flexible AC transmission system (FACTS) devices will introduce more non-linear elements into the power network and weakens the performance of conventional load flow approaches because the load flow equations will be more

nonlinear. In coping with the nonlinearity of the load models, a critical evaluation of step size optimisation based load flow methods is proposed in [38] for ill-conditioned, heavily loaded and overloaded systems. However, this method is highly sensitive to the initial settings of the variables. In [35], Zeng *et al*. proposed a very interesting method to estimate the maximum loading conditions by using the voltages from a set of operating points, obtained by conventional load flow calculations along a predefined load increase direction. The method is based on analysis of Jacobian matrix behaviour near the maximum loading point, where it becomes singular [39].

Recently, the utilisation of interior point methods to obtain the critical point was proposed in [40, 41, 42] . Also, many voltage collapse proximity indices were proposed, such as the one based on the Jacobian matrix minimum singular values [33]. Nonlinear programming technique has been proposed in [31] to determine the MLP efficiently. Sensitivity techniques have shown to be very useful for determining the voltage stability margins, which can be given in terms of MW, Mar or MVA [32, 42, 43]. Other research works have focused on maximizing the real power transfer before voltage collapse occurs, for instance, after a strategic reactive load allocation [42]. The real power losses minimisation has been utilised to increase the loadability of power systems in [44].

Security margins to voltage collapse in parameter space provide important analysis information and can be determined by simple computational procedures

while maintaining a good accuracy. Several algorithms have been developed to detect how close a system is to voltage collapse [36, 44, 45]. All these algorithms assess the distance between the present loading and the maximum loading point in parameter space.

1.4.2 MLP Determination during Contingency

Voltage security is becoming increasingly important in electric power systems. A fast and accurate solution is in demand to perform the analyses efficiently for a numerous number of contingencies online. Various methods have been proposed so far for voltage stability evaluation. For example, a series of methods [46]-[49] have been proposed to predict the load power margins for post-contingency systems based on the sensitivity analysis of the pre-contingency system. Another approach, known as look-ahead method is used to predict post-contingency conditions based on a quadratic curve fit [50]. The use of the reactive power reserves has been proposed as an index to evaluate the voltage stability of post-contingency systems [51]. .

Other stability indices have been proposed based on the second order information derived from the singular value analysis of the power flow Jacobian in [98]. Furthermore, the relations between voltages and local reactive supports have been utilised to propose a stability index in [52].. In [98], A. J. Flueck

proposes a new power sensitivity method of ranking branch outage contingencies for voltage collapse. The distinguishing features of the method are the ability to rank all branches in a large-scale power system quickly and to estimate the outage contingency bifurcation values accurately. These previous studies are mainly for branch outage contingencies. The idea of calculating MLP during generator outage was recently proposed in [53] and is an important area of work.

1.5 Proposed Approach

In this thesis, a load flow method based on Evolutionary Algorithm (EA) has been proposed. Two prominent EAs are adopted in this investigation, which are Genetic Algorithm and Particle Swarm Optimisation algorithms. A Constrained Genetic Algorithm (CGA) load flow method was developed by Wong, Li and Law in [54] and its robustness and efficiency was enhanced using the concept of virtual population and solution acceleration techniques developed in [55]. The enhanced CGA is referred to as the Advanced Constrained Genetic Algorithm (ACGA) load flow algorithm. The solution acceleration techniques in ACGA consist of the nodal voltage differential technique and the gradient acceleration technique.

The PSO algorithm is incorporated into the framework of ACGA to enhance the quality of solution in terms of speed of convergence and accuracy. The developed method is so called as hybrid CGA / PSO, which prove to be

efficient in solving benchmark power system problems. Their solution process does not rely on the starting values of the variables. The proposed algorithm has been found to have the capability to determine both the normal and abnormal load flow solutions of a number of IEEE test systems. It has also been found that this load flow algorithm can determine the load flow solution at the maximum power loading point with only a few iterations. The numerical improvements in terms of speed of convergence, capability of finding greater maximum loading point are being reported in this thesis.

1.6 Layout of Thesis

Chapter 1, which is this chapter, presents the literature review of the subjects concerned in this thesis. The framework of the proposed approach is also described in this chapter, given the details of the background of the newly developed algorithm in this thesis.

Chapter 2 gives a brief review of Evolutionary Algorithms and Particle Swarm Optimisation. This includes explanation on Particle Swarm Optimisation and hybrid Evolutionary Algorithms. The common architecture of hybrid algorithm is also discussed, including the survey of hybrid PSO / EA algorithms.

Chapter 3 elaborates the proposed algorithm, hybrid CGA/PSO in solving the load flow problem. The flow of the algorithm is also available. Problem formulation of the load flow problem is also given in this chapter.

Chapter 4 presents the preliminary investigation of Hybrid CGA/PSO load flow algorithm. The parameter sensitivity analyses are carried out to determine the best setting values for optimal performance of the proposed hybrid algorithm.

Chapter 5 investigates the performance of Hybrid CGA/PSO load flow algorithm in finding Maximum Loading Point (MLP) on IEEE test systems. Some significant results are presented in this chapter.

Chapter 6 explores the ability of the newly developed algorithm in finding and locating the Type-1 load flow solutions. As Type-1 solutions are closely related to the stability of a system, some related information on the characteristics of Type-1 solutions are concisely written.

Chapter 7 reports the application of the hybrid CGA/PSO can be applied to calculate the security margins of power system during branch or generator outage. The value of security margin provides the exact range of a system to stability boundary.

Chapter 8 provides an overall conclusion to this thesis along with suggestions for future work in this area.

Chapter 2

2. Evolutionary Algorithms and Particle Swarm Optimisation

2.1 Introduction

Evolutionary Algorithms (EAs) have become an important problem solving methodology in many fields and they have been applied to power systems. The population-based collective learning process, self-adaptation and robustness are some of the key features of evolutionary algorithms when compared to other global optimisation techniques. Although EA has been widely accepted for solving several important practical applications in engineering, very often they deliver only marginal performance. Inappropriate selection of various parameters, representation etc. are frequently the root cause. It is quite impossible that one could find a uniformly best algorithm to solve all optimisation problems. This is in accordance with the No Free Lunch theorem, which explains that for any algorithm, any elevated performance over one class of problems is exactly paid for in performance of another class. Recently, hybridisation of evolutionary algorithm is getting popular due to their

capabilities in handling several real world problems involving complexity, noisy environment, imprecision, uncertainty and vagueness. In this chapter, the background information on EAs, PSO and hybrid algorithms are presented. Also, the survey consisting of interesting hybrid frameworks of EAs and PSO algorithms are discussed.

2.2 Evolutionary Algorithms (EAs)

Evolutionary Algorithms offer practical advantages to difficult optimisation problems. These advantages are multifold; having the features of simplicity, robust response, adaptive and flexible. The evolutionary algorithm can be applied to problems where heuristic solutions are not available or generally lead to unsatisfactory results. Thus is the reason for the increased interest concerning EAs, particularly with regard to the manner in which they may be applied for practical problem. The popular algorithms under the category of EAs are numerous. Some common ones are genetic algorithms [56]-[58], evolutionary strategies [59] and evolutionary programming [60]. These algorithms share a common conceptual base on simulating the evolution of individual structures via selection, crossover and mutation. The processes may vary for different algorithm. For example, the EP algorithm does not have the process of crossover and depend mainly on mutation to create a diversified population. Compared to other global optimisation techniques, EAs are easy to

implement and very often they provide adequate solutions. The flow chart of an EA is illustrated in Figure 2.1 below.

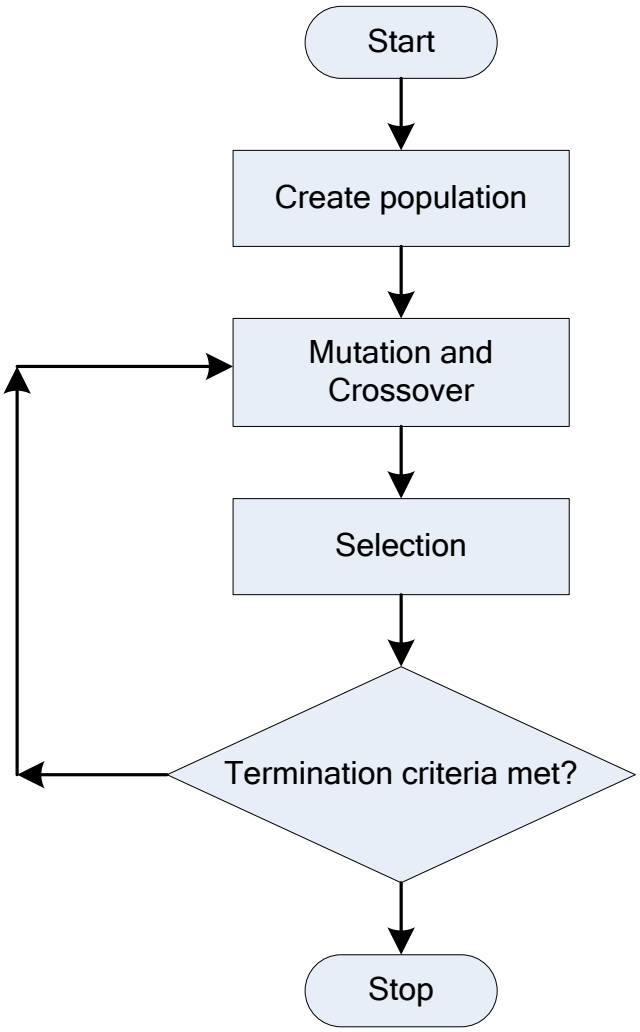

Figure 2.1: Flowchart of an Evolutionary Algorithm

From Figure 2.1, a population of candidate solutions for the optimisation process is initialised. From the initial population, new solutions are created through manipulating operators such as mutation or crossover. The fitness of the resulting solution is evaluated and suitable selection strategy is then applied to determine the survival of the candidate solutions to the next generation. The

procedure is iterated until a termination criterion is met.

2.3 Particle Swarm Optimisation

As Genetic Algorithm is now well-known and the details of Genetic Algorithm can be found in references [56]-[58], only the particle swarm optimisation (PSO) method [61] is described in this chapter. The method has been found to be able to solve optimisation problems featuring non-differentiability, high dimension, multiple optima and non-linearity. The PSO algorithm is a model that mimics the movement of individuals such as fishes, birds, or insects within a group or swarm. Similar to GA, a PSO consists of a population refining its knowledge of the given search space. PSO is inspired by particles moving around in the search space. The individuals in a PSO thus have their own positions and velocities. Each particle moves in the search space with velocity which is dynamically adjusted and balanced based on its own best movement (*pbest*) and the best movement of the group (*gbest*).

Instead of using evolutionary operators such as selection, mutation and crossover, each particle in the population moves in the search space with velocity which is dynamically adjusted. In PSO, a population consists of N particles. Each particle has d variables (dimensions) and each variable has its own range of value, velocity and position. The values, velocities and positions

of the variables are updated every iteration until maximum iteration is reached. Each particle keeps track of its coordinates in the search space, which are associated with the best solution it has achieved so far. This value is known as *pbest*. Another best value that is tracked is the overall best value or the best solution, *gbest*, in the population.

As stated, the PSO technique consists of, at each time step, changing the velocity of each particle toward its *pbest* and *gbest* solutions. The movement is weighted by a random term, with separate random numbers being generated toward *pbest* and *gbest* values. For example the *i*th particle consisting *d* dimensions is represented as $X_i = (X_{i,1}, X_{i,2}, X_{i,3}, \ldots, X_{i,d})$. The same notation applied to the velocity, $V_i = (V_{i,1}, V_{i,2}, V_{i,3}, \ldots, V_{i,d})$. The best previous position of the *i*th particle is recorded and represented as $pbest_i = (pbest_{i,1}, pbest_{i,2}, pbest_{i,3}, \ldots pbest_{i,d})$. For minimisation, the value of $pbest_i$ with lowest fitness is taken to be *gbest*. The modification of velocity and position are calculated using the current velocity and the distance from $pbest_{i,j}$ to $gbest_j$ as in:

$$V_{i,j}^{t} = wV_i^{t-1} + \rho_1 r_1 (gbest_j - X_{i,j}^{t-1}) + \rho_2 r_2 (pbest_{i,j} - X_{i,j}^{t-1}) \qquad (2.1)$$

$$X_{i,j}^{t} = X_{i,j}^{t-1} + V_{i,j}^{t} \qquad (2.2)$$

where $i \in 1...N,\ j \in 1...d, t \in 1...T$ with N is the number of population size, d is the number of dimension and T is the number of maximum generation. The

parameters ρ_1 and ρ_2 are set to constant values, which are normally given as 2.0 whereas r_1 and r_2 are two random values, uniformly distributed in [0, 1]. The constants, ρ_1 and ρ_2 represent the weighting of the stochastic acceleration terms that pull each particle toward *pbest* and *gbest* positions.

The position, X of each particle is updated for every dimension for all particles in each iteration. This is done by adding the velocity vector to the position vector, as described in eqn. (2.1) above. In eqn. (2.2), w is known as the inertia weight [62]. Suitable selection of w provides a balance between global and local explorations, thus requiring less iteration on average to find sufficiently optimal solution. Low values of w limits the contribution of the previous velocity to the new velocity, limiting step sizes and therefore, limiting exploration. On the other hand, high values result in abrupt movement toward target regions.

When applying PSO to the load flow problem, each particle is a candidate solution whereby the elements are the unknown real and imaginary parts of the power network nodal voltages.

2.4 Hybrid Evolutionary Algorithms

For several problems a simple EA might not be good enough to find the desired solution. There are several types of problems where a direct evolutionary

algorithm fails to obtain satisfactory solution [63]-[66]. This clearly paves way to the need for hybridisation of evolutionary algorithms with other optimisation algorithms, machine learning techniques, heuristics etc. Some of the possible reasons for hybridisation are as follows [67]:

1. To improve the performance of the evolutionary algorithm (e.g. speed of converge).
2. To improve the quality of the solutions obtained by EA (e.g. accuracy of result).
3. To incorporate the EA as a part of a larger system.

In 1995, Wolpert and Macready [68] illustrated that all the algorithms that search for an extreme of a cost function perform exactly the same, when averaged over all possible cost functions. In other words, if algorithm *A* outperforms algorithm *B* on some cost functions, then loosely speaking there must exist exactly as many other functions where *B* outperforms *A*. Hence, from a problem solving perspective it is difficult to formulate a universal optimisation algorithm that could solve all the problems. Hybridisation may be the key to solve some practical problems.

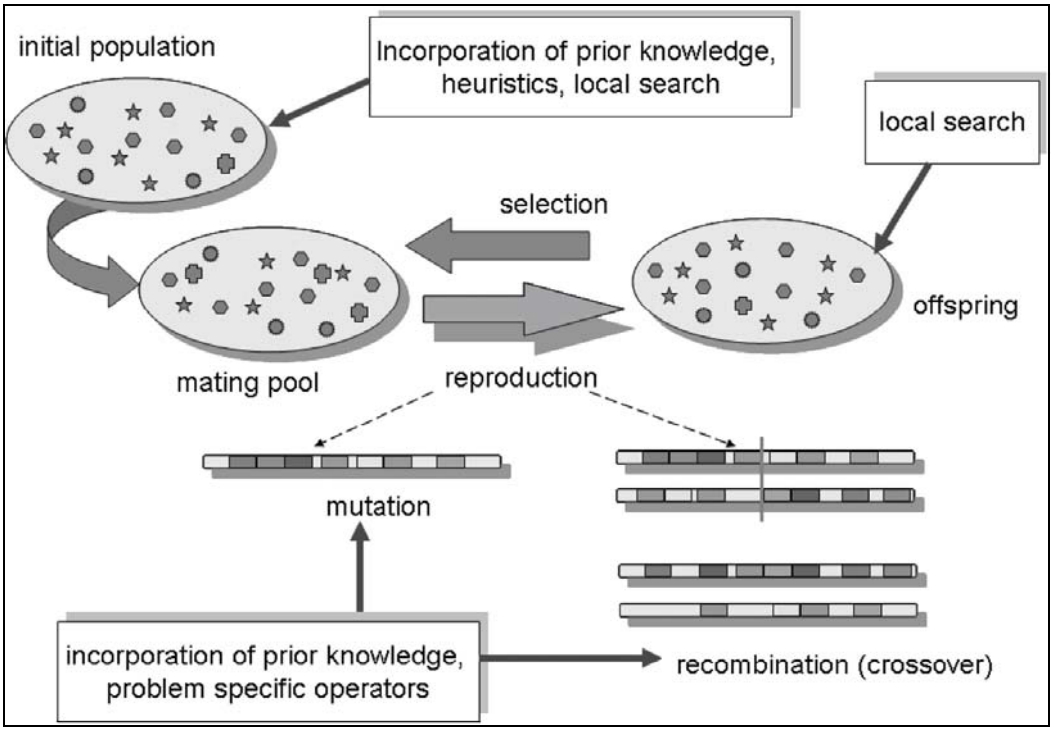

Figure 2.2: Hybridisation possibilities in an Evolutionary Algorithm

Figure 2.2 illustrates some possibilities for hybridisation. From initialisation of population to the generation of offspring, there are numerous ways to incorporate other algorithm to the original algorithm. Population may be initialised by incorporating known solutions or by using heuristics, local search etc. Local search methods may be incorporated within the initial population members or among the offspring. Evolutionary algorithms may be hybridised by using operators from other algorithms or by incorporating domain-specific knowledge. Evolutionary algorithm behaviour is determined by the exploitation and exploration relationship kept throughout the run. Adaptive evolutionary algorithms have been built for inducing exploitation/exploration relationships that avoid the premature convergence

problem and optimise the final results. The performances of the evolutionary algorithm can be improved by combining problem-specific knowledge for particular problems.

2.5 Architectures of Hybrid Evolutionary Algorithms

The integration of different learning and adaptation techniques, to overcome individual limitations and achieve synergetic effects through hybridisation or fusion of these techniques, has in recent years contributed to a large number of new hybrid evolutionary systems. Most of these approaches have unique designs, further justified by success in certain application domains. Due to the lack of a common framework, it remains often difficult to compare the various hybrid systems conceptually and evaluate their performance comparatively. There are several ways to hybridise a conventional evolutionary algorithm for solving optimisation problems. Some of them are summarised below [69]:

i. The solutions of the initial population of EA may be created by problem-specific heuristics.
ii. Some or all the solutions obtained by the EA may be improved by local search. These algorithms are known as mimetic algorithms [70, 71].
iii. Solutions may be represented in an indirect way and a decoding algorithm maps any genotype to a corresponding phenotypic solution. In this

mapping, the decoder can exploit problem-specific characteristics and apply heuristic etc.

iv. Variation operators may exploit problem knowledge. For example, in recombination more promising properties of one parent solution may be inherited with higher probabilities than the corresponding properties of the other parent(s). Also mutation may be biased to include in solutions promising properties with higher probabilities than others.

2.6 Hybrid Evolutionary Algorithms / Particle Swarm Optimisation

PSO incorporates swarming behaviours observed in flocks of birds, schools of fish, or swarm of bees, and even human social behaviour, from which the idea originated [72]-[75]. A hybrid evolutionary algorithm / PSO is proposed by Shi et al. [76]. The hybrid approach executes the two systems simultaneously and selects P individuals from each system for exchanging after the designated *N* iterations. The individual with larger fitness has higher probability to be selected.

Another hybrid technique combining GA and PSO known as genetic swarm optimisation (GSO) is proposed by Grimaldi et al. [77] for solving an electromagnetic optimisation problem. The method consists of a strong co-operation of GA and PSO, since it maintains the integration of the two techniques for the entire run. In each iteration, the population is divided into

two parts and they evolved with the two techniques, respectively. They are then recombined in the updated population, that is again divided randomly into two parts in the next iteration for another run of genetic or particle swarm operators. The population update concept can be easily understood whereby a portion of the individuals is substituted by new generated ones by means of GA, while the remaining are the same as the previous generation, manipulated by PSO.

Grosan et al. [78] proposed a variant of the PSO technique named independent neighbourhoods particle swarm optimisation (INPSO) dealing with subswarms for solving the well known geometrical place problems. The performance of the INPSO approach is compared with Geometrical Place Evolutionary Algorithms (GPEA). The main advantage of INPSO technique is its speed of convergence. To enhance the performance of the INPSO approach, a hybrid algorithm combining INPSO and GPEA is also proposed in this paper. The developed hybrid combination is able to detect the geometrical position much faster even for difficult problems whereby the direct GPEA approach required more computational cost and the INPSO approach failed in finding all the geometrical position points.

Liu et al. [79] introduced turbulence in the particle swarm optimisation (TPSO) algorithm to overcome the problem of stagnation. The algorithm used a minimum velocity threshold to control the velocity of particles. TPSO

mechanism is similar to a turbulence pump, which supplies some power to the swarm colony to explore new neighbourhoods for better solutions. The algorithm avoids clustering of particles and attempts to maintain diversity of population. The maximum velocity (V_{max}) of particles is tuned adaptively by FLCs in the TPSO algorithm, which is named as Fuzzy Adaptive TPSO (FATPSO). The comparison was performed on a suite of 20 widely used benchmark problem.

2.7 Conclusions

As evident from the scientific literature, the use of hybrid evolutionary algorithms are getting very popular. In this chapter, the various possibilities for hybridisation of an evolutionary algorithm are illustrated. The generic hybrid evolutionary architectures that have evolved during the last couple of decades are also presented. The survey of some interesting works on hybrid EA and PSO reported in literature has been discussed.

Chapter 3

3. Hybrid CGA / PSO Load Flow Algorithm

3.1 Introduction

Hybrid algorithms as been a hot topic in current research trend [65, 76, 77, 78, 80]. Depending on the optimisation problem, each hybrid algorithm developed is unique, utilising different architectures as explained in Section 2.5. Following the same principle, a hybrid algorithm based on Genetic Algorithm (GA) and Particle Swarm Optimisation (PSO) algorithms is developed in this thesis. The PSO is incorporated into the existing framework, which is Constrained Genetic Algorithm (CGA). In addition, as the developed algorithm aims to solve load flow problem, therefore, this developed algorithm is called hybrid CGA/PSO load flow algorithm. In this chapter, the formulation of the load flow problem is presented. This is followed by the details on hybrid CGA/PSO load flow algorithm. The flow of the algorithm developed is also described. Then, the conclusion is derived.

3.2 Load Flow Problem Formulation

In interconnected n node power system, there are N_{PQ} load nodes, N_{PV} voltage-controlled nodes and one slack bus. In rectangular coordinates, there are 2(n-1) unknowns to find. These unknowns are the voltages of the load nodes, the voltage angles and the reactive power at the generator nodes. The load flow problem in this context can be formulated as nonlinear optimisation problem [54] that is the minimisation of the objective function results from the summation of squares of the power mismatches and voltage mismatches. At any node i the nodal active power, P_i and reactive power, Q_i are given as follows:

$$P_i = E_i \sum_{j=1}^{n} (G_{ij}E_j - B_{ij}F_j) + F_i \sum_{j=1}^{n} (G_{ij}F_j + B_{ij}E_j) \tag{3.1}$$

$$Q_i = F_i \sum_{j=1}^{n} (G_{ij}E_j - B_{ij}F_j) - E_i \sum_{j=1}^{n} (G_{ij}F_j + B_{ij}E_j) \tag{3.2}$$

where G_{ij} and B_{ij} are the (i, j)th element of the admittance matrix. E_i and F_i are real and imaginary part of the voltage at node i. If node i is a PQ-node where the load demand is specified, then the mismatches in active and reactive powers, ΔP_i and ΔQ_i respectively, are given by:

$$\Delta P_i = \left| P_i^{sp} - P_i \right| \tag{3.3}$$

$$\Delta Q_i = \left| Q_i^{sp} - Q_i \right| \tag{3.4}$$

in which P_i^{sp} and Q_i^{sp} are the specified active and reactive powers at node i. When node i is a PV-node, the magnitude of the voltage, V_i^{sp} and the active

power generation at node *i* are specified. The mismatch in voltage magnitude at node *i* can be defined as:

$$\Delta V_i = \left| V_i^{sp} - V_i \right| \tag{3.5}$$

In eqn. (3.5), V_i is the calculated nodal voltage at PV-node *i* and is given by:

$$V_i = \sqrt{E_i^2 + F_i^2} \tag{3.6}$$

Apart from solving the load flow problem by the conventional methods, the problem can be viewed as an optimisation problem, in which an objective function *H* is to be minimised:

$$H = \sum_{i \in N_{pq}+N_{pv}} \Delta P_i^2 + \sum_{i \in N_{pq}} \Delta Q_i^2 + \sum_{i \in N_{pv}} \Delta V_i^2 \tag{3.7}$$

where N_{pq} and N_{pv} are the total numbers of PQ-nodes and PV-nodes respectively. When the load flow problem is solvable, the value of *H* is zero or in the vicinity of zero at the end of the optimisation process. If the problem is unsolvable, the value of *H* will be greater than zero.

In the minimisation process, the fitness or the degree of goodness of the particle as a candidate solution is measured by means of the following fitness function *F* [55]:

$$F = \frac{1}{10^{-5} + 2H - H_{av}} \tag{3.8}$$

where H_{av} is the average of mismatches representing the measure of the evenness of the spread of mismatch values throughout the nodes and is calculated from:

$$H_{av} = \frac{\sum_{i=2}^{n} \Delta P_i}{n_{pv} + n_{pq}} + \frac{\sum_{i \in n_{pq}} \Delta Q_i}{n_{pq}} \qquad (3.9)$$

3.3 Hybrid CGA/PSO Load Flow Algorithm

A Constrained Genetic Algorithm (CGA) load flow method was reported in [54] and its robustness and efficiency was enhanced using the concept of virtual population and solution acceleration techniques developed in [55] and is one of the earliest hybrid evolutionary algorithm developed for solving power engineering problems. The enhanced CGA is referred to as the Advanced Constrained Genetic Algorithm (ACGA) load flow algorithm. The solution acceleration techniques in ACGA consist of the nodal voltage differential technique and the gradient acceleration technique. The ACGA algorithm has been found to have the capability to determine both the normal and abnormal load flow solutions of a number of IEEE test systems. It has also been found that ACGA can determine the load flow solution at the maximum power loading point with only a few iterations.

While the details of ACGA can be found in [55], the framework of the ACGA is shown here in Figure 3.1. In this framework, a virtual population consists of the current population of candidate load flow solutions and two new populations, A and B, derived from the current population using the nodal voltage differential solution acceleration method. Population A is derived by

accelerating candidate solutions in the current population towards the best candidate solution in the same population. On the other hand, population B is formed by accelerating candidate solutions away from the best candidate solution in the population. The current population, population A and population B are then combined to form population C. The resultant population is formed from population C with twenty-five percent of its candidate solutions accelerated by means of the gradient technique. The resultant population is then used as the current population in the evolutionary cycle.

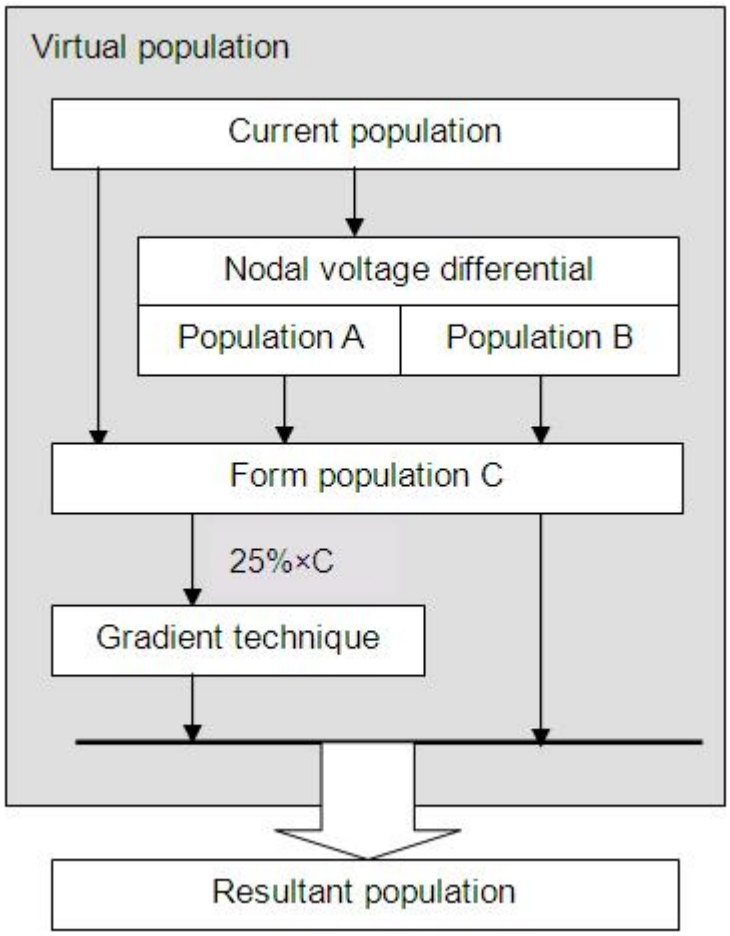

Figure 3.1: Formation of virtual and resultant populations of candidate solutions in ACGA

It can be observed that the nodal voltage differential acceleration technique employed in ACGA is not general enough. This technique only upgrades the candidate solutions in two opposite directions. But there is no guarantee that upgrading along these directions will help the evolutionary optimisation process.

In this thesis , it is proposed to employ the Particle Swarm Optimisation (PSO) technique [61] to replace the nodal voltage differential acceleration technique in ACGA as shown in Figure 3.2, because the PSO can upgrade the

candidate solutions in many different directions and hence cover a bigger search space than the voltage differential acceleration method. The use of PSO here can also be viewed as a method of mutation in the genetic algorithm process. Hence, to prevent any good candidate solutions from being destroyed by the PSO technique, the technique is only applied subject to a 'mutation probability' setting as indicated by *mp*% in Figure 3.2. With this arrangement, the resultant algorithm can be viewed as a hybrid Constrained GA/PSO algorithm for solving the load flow problem. Because of the more general nature of this new hybrid algorithm, it should be more powerful than its predecessor ACGA and should be capable of obtaining better load flow solution values particularly when the power system is very heavily loaded. It is, however, emphasised here that the new algorithm is a powerful alternative when conventional methods fail to find the load flow solution. It is also noted here that although PSO has been used in solving power system optimisation problems [81]-[83], it has not been employed in the way described in this thesis.

The procedure of the proposed hybrid CGA/PSO load flow algorithm is given in the following:

1. Initialise the particles, consisting of the real and imaginary parts of the nodal voltages of the candidate solutions in the population.
2. Evaluate the fitness of all particles using eqn (3.8).

3. Generate new population of candidate solutions using roulette-wheel selection, 2-point crossover and PSO mutation.
4. Perform the constraint satisfaction process on the candidate solutions in the new population for the generator nodes and load nodes as described in [54].
5. Accelerate 25% of the constrained candidate solutions using the gradient technique in[55].
6. Update the best solution.
7. Go to step 2 until the termination criterion is met.

In step 3 above, the PSO algorithm is applied as a mutation strategy. The optimal mutation probability is found through parameter sensitivity analysis in chapter 3. The algorithm will terminate when all the power mismatches of the PQ nodes are within the preset tolerance, otherwise it will terminate on reaching the maximum allowable number of evolutionary generations. This termination criterion is employed in step 7 of the above procedure.

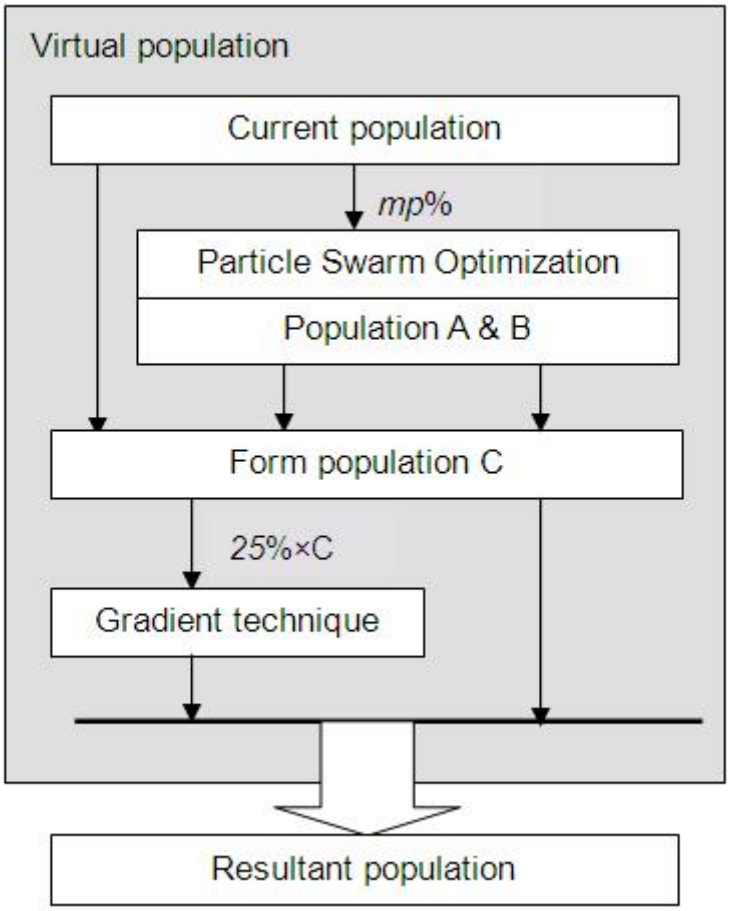

Figure 3.2: The proposed framework showing the formation of virtual and resultant populations of candidate solutions

3.4 Conclusions

In the development of hybrid CGA/PSO, the PSO algorithm has been incorporated as a mutation replacing the conventional mutation in the GA algorithm. The framework of the proposed algorithm is graphically illustrated, showing the role of PSO algorithm in replacing the acceleration techniques in existing ACGA. The following chapter describes the tuning of parameter through some sensitivity analyses to determine the optimal values for the relevant parameters in the hybrid algorithm.

Chapter 4

4. Parameter Settings in Hybrid CGA/PSO Algorithm

4.1 Introduction

Like other optimisation methods, the performance of the CGA/PSO algorithm depends on the settings of its parameters. This chapter reports the parameter sensitivity analysis carried out for the hybrid CGA/PSO algorithm for finding load flow solutions. In the PSO methods, there are several parameters to be set. In order to use the PSO efficiently, the value ranges of these parameters should be investigated for solving the load flow problem. The experimental approach and parametric sensitivity analyses in finding the appropriate value ranges of the PSO coefficients are also reported. The power of the new hybrid algorithm is demonstrated by the application of the new algorithm to determine the heavy loading cases of several test systems.

4.2 Parameter Settings of PSO

PSO has several parameters, which are the number of particles in the swarm (N), inertia weight (w), maximum velocity (V_{max}), the parameter for attraction towards *pbest* and *gbest* (ρ_1 and ρ_2). In this thesis, the parameters ρ_1 and ρ_2 are set to constant values, which are commonly set as 2.0. The constants, ρ_1 and ρ_2 represent the weighting of the stochastic acceleration terms that pull each particle toward *pbest* and *gbest* positions, acting as the cognitive and social parameters respectively. The r_1 and r_2 are two random values, uniformly distributed in [0, 1]. To prevent any undesirable exploration of a particle along a given dimension, the velocity may be restricted by a constriction coefficient [84] but this yields negative effects [85]. Instead of using a constriction coefficient, the velocity in a dimension is restricted by the maximum velocity (V_{max}). This keeps the random search of potential solutions within control. The value of V_{max} in this thesis is 10% of the search range, which is the best value from empirical study for the load flow problem. Other parameters such as inertia weight (w) and population size (N) are found from the parameter sensitivity analysis presented in the following section. The common parameter settings for both algorithms are as shown in Table 4.1. Other parameters concerned are given in Table 4.2.

Table 4.1: Common parameter settings for ACGA and Hybrid CGA/PSO

Parameter	Settings
Active and reactive power tolerance	0.001 p.u. on 100MVA base
Gradient acceleration, G	25% of the population
Number of trials	50
Maximum Generation, T	150
Voltage initialisation range	$0.9 < V < 1.2$ and $-30° < \theta < 0°$
Population size, N	8

Table 4.2: Other parameter settings for ACGA and Hybrid CGA/PSO

Parameter	ACGA	Hybrid CGA/PSO
Crossover rate	Two-point crossover	Two-point crossover
Selection strategy	Roulette Wheel	Roulette Wheel
Mutation mp	Uniform mutation with $mp = 0.01$	PSO mutation with $mp = 0.5$
Inertia weight w	-	0.1
Maximum Velocity V_{max}	-	10% of search space

4.3 Experimental Settings

In determining the inertia weight (w), population size (N) and the mutation probability (mp) by sensitivity analysis for the proposed hybrid algorithm, the IEEE 30-, 57- and 118-bus systems are used [104] and the algorithm is run with different parameter settings. The settings given in Tables 4.1 and 4.2 are applied to all the experiments. The algorithm is executed on a 3.0 GHz Pentium IV computer. The results of these experiments will be presented in tables with the

column containing the attributes as follows:

Ave Time : Average time taken to complete a trial. Only successful trials are considered.

Ave Iter : The average iteration for a trial which is successful.

S.R. : A trial is considered successful if all nodes value is within the tolerance before maximum generation, *T* is reached.

Std Dev : This is standard deviation. A small standard deviation denotes that the algorithm is stable.

Best : The best results obtained within all successful trials.

Average : Average of all trials. Only successful trials are taken into account.

Worst : The worst result among all successful trials

4.4 Effect of inertia weight (*w*) in PSO equations

The value of inertia weight, *w* is in the range of 0 to 1. In determining the best value of *w* for the load flow problem *w* is varied from 0.1 until 0.9 with a step increment of 0.1 as shown in Figure 4.1. In this figure, the case of IEEE 118-bus system is illustrated. The numerical results are tabulated in Table 4.3 and illustrated by the relevant curves in Figure 4.1, representing the average iteration, average time and success rate. From this graph, the average time and average iteration increase with respect to higher value of *w* while at the same

time, the success rate decreases. In other words, the success rate (S.R.) deteriorates as the value of inertia weight increases.

It seems that smaller value of *w* is more efficient as this guarantees better reliability and cheaper computational cost. Therefore, *w*=0.1 is adopted as the best setting for future analysis, highlighted in Table 4.3 below. The similar analysis has been carried out on IEEE 30- and 57- bus systems. The graphs plotted from the results of IEEE 30-bus system are given in Figures 4.2 and 4.3. From simulation, the same value for *w* is concluded in these analyses, depicted in Table 4.4. From the simulation involving *w*<0.1, it is found that setting *w*<0.1 has slightly lower performance compared to *w*=0.1.

Table 4.3: Parameter sensitivity analysis for inertia weight (*w*) with 60% load increment on IEEE 118-bus system

w	Ave Iter	Ave Time[s]	S.R. (%)	Std Dev	H		
					Best	Average	Worst
0.1	**9**	**3.64**	**94**	**1.15×10^{-6}**	**0**	**1.06×10^{-6}**	**5.0×10^{-6}**
0.2	14	5.26	88	1.10×10^{-6}	0	1.11×10^{-6}	4.0×10^{-6}
0.3	18	7.18	76	9.35×10^{-7}	0	1.13×10^{-6}	3.0×10^{-6}
0.4	21	8.35	62	1.21×10^{-6}	0	1.26×10^{-6}	4.0×10^{-6}
0.5	25	9.37	62	1.36×10^{-6}	0	1.23×10^{-6}	5.0×10^{-6}
0.6	28	10.7	78	1.36×10^{-6}	0	1.80×10^{-6}	6.0×10^{-6}
0.7	36	17.1	66	1.41×10^{-6}	0	1.76×10^{-6}	6.0×10^{-6}
0.8	47	17.2	62	1.51×10^{-6}	0	1.68×10^{-6}	6.0×10^{-6}
0.9	68	26.1	66	1.36×10^{-6}	0	1.33×10^{-6}	5.0×10^{-6}
1.0	91	35.0	42	1.80×10^{-6}	0	2.57×10^{-6}	6.0×10^{-6}

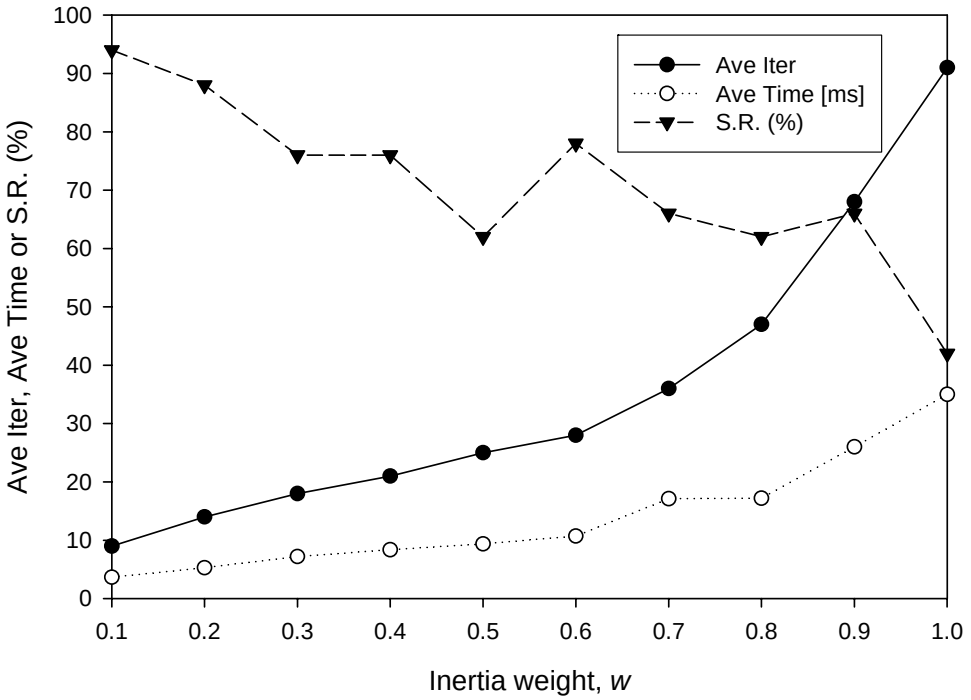

Figure 4.1: Effects of inertia weight w (0.1 to 1.0): case of IEEE 118-bus system with 60% load increment.

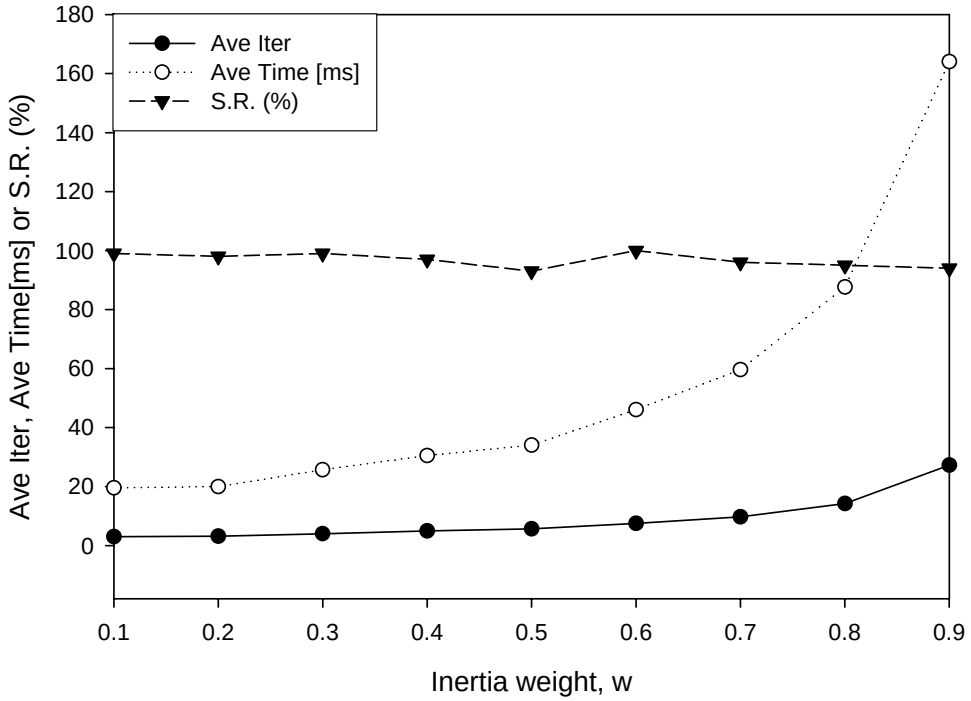

Figure 4.2: Effects of inertia weight *w* (0.1 to 1.0): case of IEEE 30-bus system with normal load.

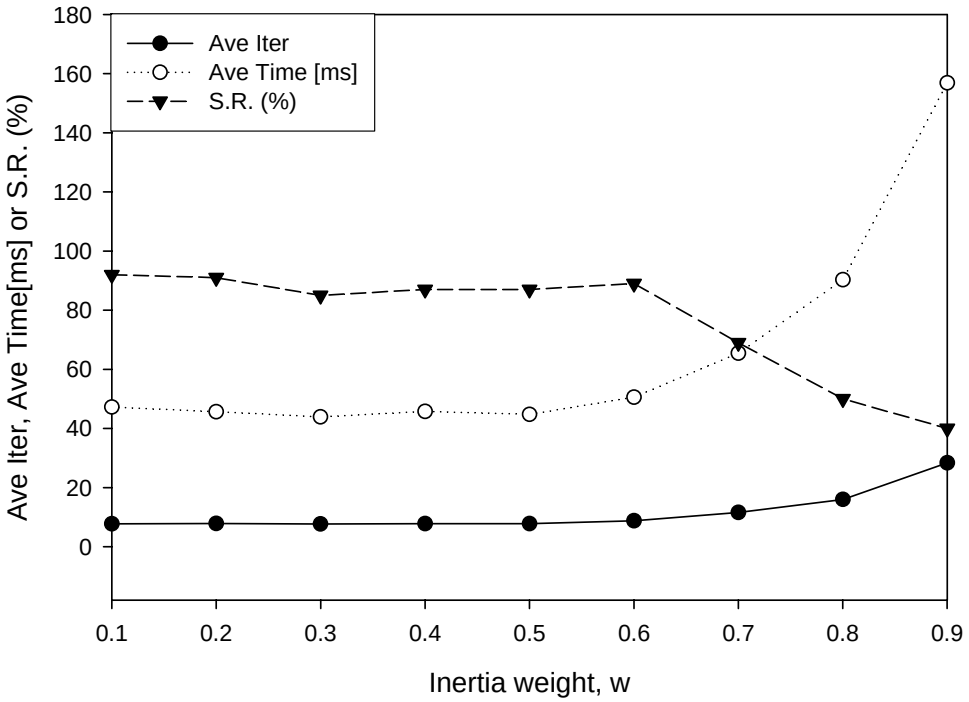

Figure 4.3: Effects of inertia weight *w* (0.1 to 1.0): case of IEEE 30-bus system with 52.04% load increment.

Table 4.4: Inertia weight (*w*) obtained via parameter sensitivity analysis

System	IEEE 30-bus	IEEE 57-bus	IEEE 118-bus
w	0.1	0.1	0.1

4.5 Effect of Population size (*N*)

The effect of the population size on hybrid CGA/PSO is investigated by varying the size from 4 to 40. The numerical results are recorded in Table 4.5 with the relevant graph plotted in Figure 4.4, showing the average iteration, average time and the success rate obtained. From this graph, a larger population size contributes to results with higher success rate. However, the

drawback of higher population size is the increment of the computational cost, as can be observed from the graph.

Table 4.5: Parameter sensitivity analysis for population size with 60% load increment on IEEE 118-bus system

Pop Size	Ave Iter	Ave Time[s]	S.R. (%)	Std Dev	H		
					Best	Average	Worst
4	11.0	2.34	62	1.63×10^{-6}	0	1.39×10^{-6}	7.0×10^{-6}
8	11.0	5.70	84	1.31×10^{-6}	0	1.19×10^{-6}	6.0×10^{-6}
12	9.6	7.41	88	1.28×10^{-6}	0	1.27×10^{-6}	5.0×10^{-6}
16	**9.8**	**9.07**	**94**	$\mathbf{1.30\times10^{-6}}$	**0**	$\mathbf{1.13\times10^{-6}}$	$\mathbf{6.0\times10^{-6}}$
20	8.5	11.0	90	1.02×10^{-6}	0	1.33×10^{-6}	4.0×10^{-6}
24	9.3	14.6	86	8.15×10^{-7}	0	9.53×10^{-7}	2.0×10^{-6}
28	8.6	19.1	94	1.20×10^{-6}	0	9.57×10^{-7}	5.0×10^{-6}
32	9.0	19.0	90	9.41×10^{-7}	0	1.02×10^{-6}	3.0×10^{-6}
36	10.0	23.6	96	1.33×10^{-6}	0	9.38×10^{-7}	6.0×10^{-6}
40	8.5	24.9	96	1.03×10^{-6}	0	1.15×10^{-6}	3.0×10^{-6}

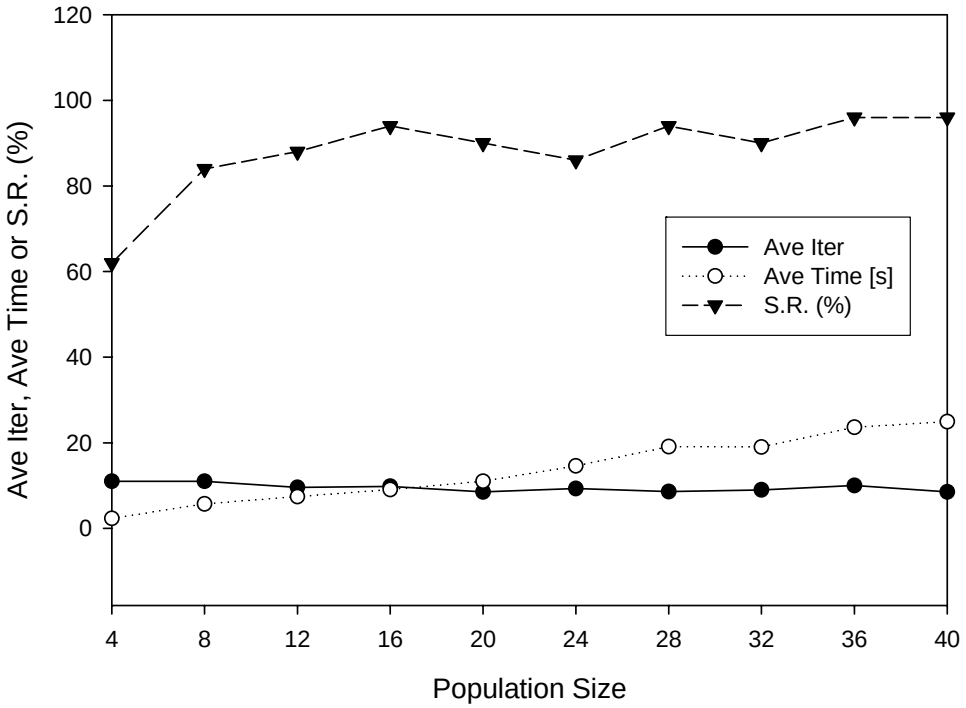

Figure 4.4: Effect of population size: case of IEEE 118-bus system with 60% load increment.

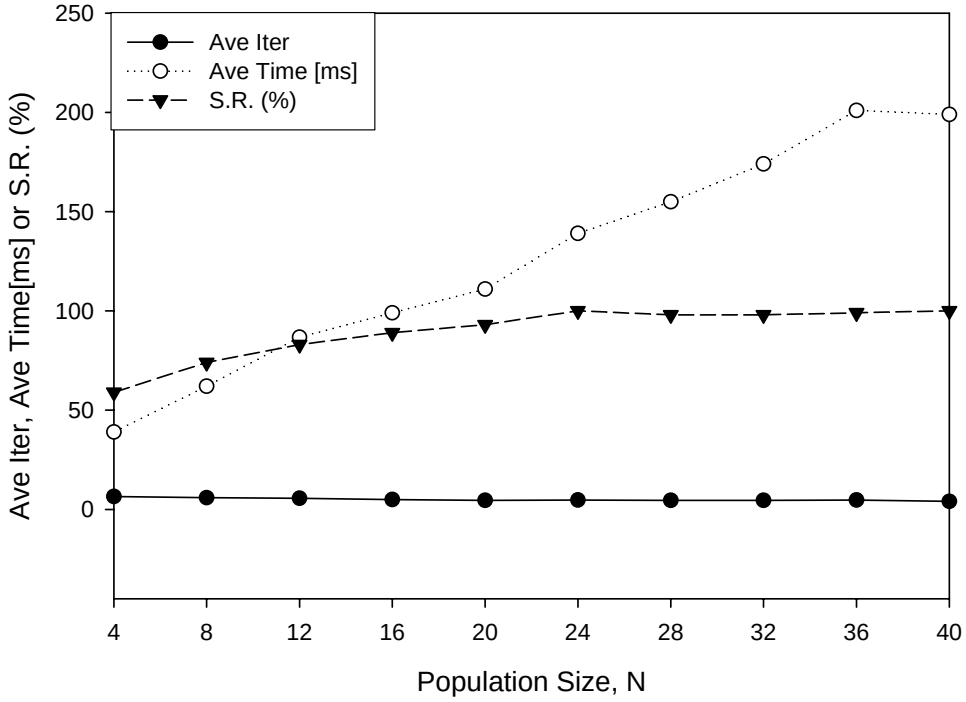

Figure 4.5: Effects of population size *N*: case of IEEE 30-bus system with normal load

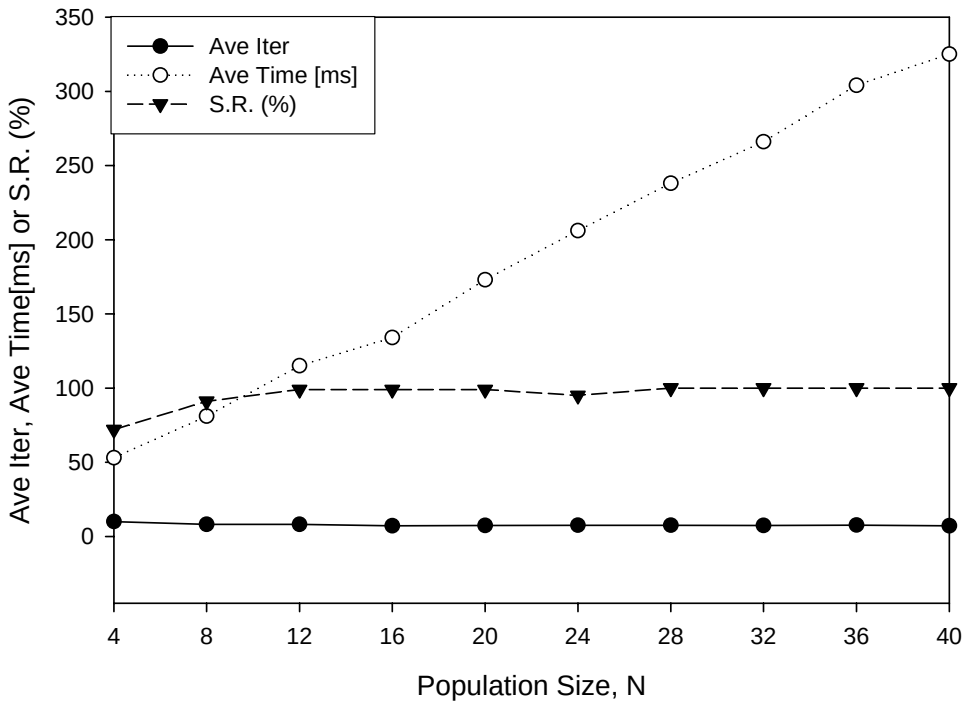

Figure 4.6: Effects of population size *N*: case of IEEE 30-bus system with 52.04% load increment.

From Figure 4.4 the curve of success rate seems to reach a stable stage with a specific population size. Hereby, we name this as “stable population size”. For the IEEE 118-bus system in Figure 4.4, the adopted population size is 16, the point given by the crossover point of the iteration and time curves in the figure. The same analysis is performed for other test systems with the preferred population sizes summarised in Table 4.6. The results on IEEE 30-bus system are plotted in Figures 4.5 and 4.6. It can be observed that for system with 30 buses, a small stable population size of 8 is appropriate. This stable population size increases for larger system with 12 and 16 population sizes for 57-bus system and 118-bus system respectively.

Table 4.6: Stable population size obtained via parameter sensitivity analysis

System	IEEE 30-bus	IEEE 57-bus	IEEE 118-bus
Pop Size	8	12	16

4.6 Mutation Probability (*mp*)

This mutation rate denotes the degree of contribution from PSO algorithm for efficient search as this is implemented as mutation in the proposed hybrid CGA/PSO algorithm. The parameter sensitivity analysis for *mp* is carried out to find the best value for the best performance of the proposed hybrid method. The mutation probability, *mp* is set from 0.1 to 1.0 with step increment size of 0.1 in parameter sensitivity analysis. Results are shown in Table 4.7 with the relevant graphs in Figure 4.9 for the case of the IEEE 118-bus test system. From the table, the best *mp* value is 1.0 when the mean iteration is 6.1 within 3.07s. The success rate recorded in this case is 94%, which is the highest among all the *mp* values, highlighted in Table 4.7. The graph showing the relevant information versus the mutation probability *mp* is shown in Figure 4.7.

Table 4.7: Parameter sensitivity analysis for mutation probability (*mp*) with 60% load increment on IEEE 118-bus system (50 Trials)

mp	Ave Iter	Ave Time[s]	S.R. (%)	Std Dev	*H*		
					Best	Average	Worst
0.1	9.7	6.19	88	1.06×10^{-6}	0	1.00×10^{-5}	5.0×10^{-6}
0.2	10	5.98	88	1.50×10^{-6}	0	1.48×10^{-6}	7.0×10^{-6}
0.3	9.6	5.46	82	1.42×10^{-6}	0	1.32×10^{-6}	5.0×10^{-6}
0.4	9.7	4.51	84	5.84×10^{-6}	0	1.88×10^{-6}	3.8×10^{-5}
0.5	7.2	4.78	84	1.45×10^{-6}	0	1.19×10^{-6}	5.0×10^{-6}
0.6	6.5	3.33	82	1.08×10^{-6}	0	1.22×10^{-6}	5.0×10^{-6}
0.7	6.4	3.56	86	7.83×10^{-7}	0	6.51×10^{-7}	3.0×10^{-6}
0.8	6.3	2.81	86	3.24×10^{-7}	0	1.16×10^{-7}	1.0×10^{-6}
0.9	6.3	3.32	86	1.52×10^{-7}	0	2.33×10^{-8}	1.0×10^{-6}
1.0	**6.1**	**3.07**	**94**	$\mathbf{5.83\times10^{-7}}$	**0**	$\mathbf{8.51\times10^{-8}}$	$\mathbf{4.0\times10^{-6}}$

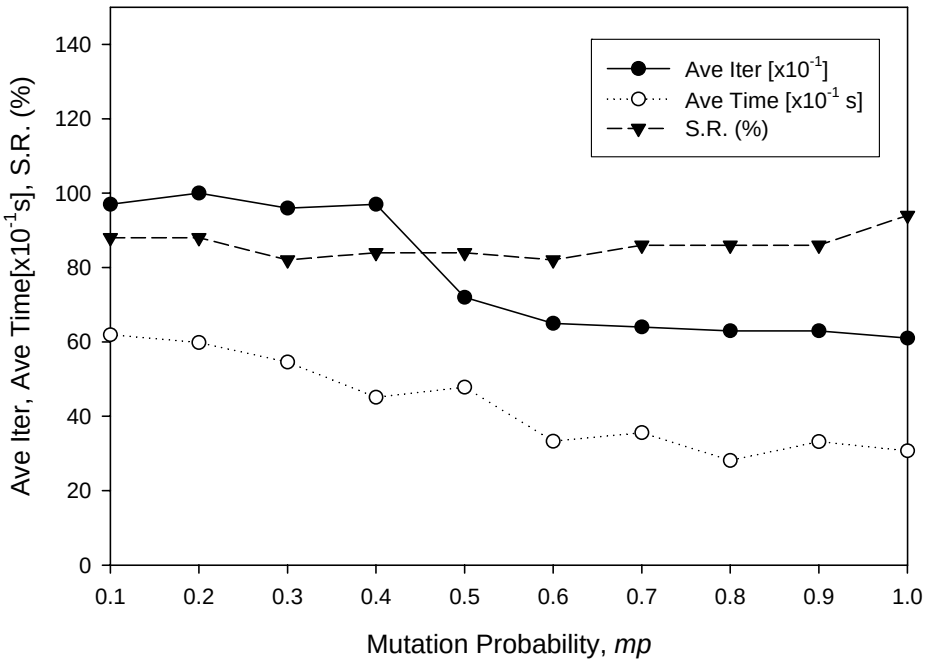

Figure 4.7: Effect of mutation probability (*mp*): case of IEEE 118-bus system with 60% load increment.

As different power systems may exhibit different behaviours, therefore, the similar parameter analysis as in Table 4.7 is carried out for other systems to obtain the appropriate value of mutation probability for each system in the aim of obtaining optimal performance. The best values obtained for other IEEE test systems are summarised in Table 4.8 below. It can be observed, a setting of 0.4 suffices for small systems and 1.0 for larger systems.

Table 4.8: Mutation probability (*mp*) obtained via parameter sensitivity analysis

System	IEEE 30-bus	IEEE 57-bus	IEEE 118-bus
mp	0.4	0.4	1.0

4.7 Effect of r_1 and r_2 in PSO equation

This analysis investigates the role of r_1 and r_2 in PSO algorithm in searching for the solution. In the original form of PSO, these values are uniformly distributed between [0, 1]. However, in this analysis, a series of ranges for r_1 and r_2 are investigated as observed in Tables 4.9 and 4.10.

Table 4.9: Parameter sensitivity analysis for r_1 and r_2 on IEEE 30-bus system for normal load

r_1, r_2	*Ave Iter*	*Ave Time*[s]	*S.R.* (%)	*Std Dev*	*H*		
					Best	*Average*	*Worst*
r[0, 1], *r*[0, 1]	5.40	0.058	84	9.26×10^{-7}	0	2.38×10^{-7}	6.0×10^{-6}
0, *r*[0, 1]	6.57	0.068	89	8.0×10^{-7}	0	2.02×10^{-7}	4.0×10^{-6}
r[0, 1], 0	5.39	0.058	70	7.36×10^{-7}	0	2.57×10^{-7}	4.0×10^{-6}
r[0, 0.5], *r*[0, 0.5]	5.77	0.062	88	5.98×10^{-7}	0	1.82×10^{-7}	3.0×10^{-6}
r[0.5, 1], *r*[0.5, 1]	6.18	0.067	77	8.77×10^{-7}	0	3.12×10^{-7}	4.0×10^{-6}

Table 4.10: Parameter sensitivity analysis for r_1 and r_2 on IEEE 30-bus system for 152.04%×normal load

r_1, r_2	*Ave Iter*	*Ave Time*[s]	*S.R.* (%)	*Std Dev*	*H*		
					Best	*Average*	*Worst*
r[0, 1], *r*[0, 1]	8.81	0.090	93	1.09×10^{-6}	0	2.13×10^{-6}	5.0×10^{-6}
0, *r*[0, 1]	8.16	0.080	76	1.17×10^{-6}	0	2.25×10^{-6}	5.0×10^{-6}
r[0, 1], 0	8.12	0.083	95	1.10×10^{-6}	0	2.27×10^{-6}	5.0×10^{-6}
r[0, 0.5], *r*[0, 0.5]	7.47	0.078	92	7.44×10^{-7}	1.0×10^{-6}	2.13×10^{-6}	5.0×10^{-6}
r[0.5, 1], *r*[0.5, 1]	9.73	0.099	97	1.14×10^{-6}	0	2.04×10^{-6}	5.0×10^{-6}

The results shown in Table 4.9 do not show a similar pattern in comparison to the results in Table 4.10. The results do not differ significantly from one and other. Further analysis on r_1 and r_2 shows that keeping r_1 and r_2 to its original form (first row of Tables 4.9 and 4.10) is the best setting.

4.8 Effect of the limit of the velocity (vel_{max} and vel_{min})

Setting the appropriate values for vel_{max} and vel_{min} is important to enable PSO to explore the search range effectively. As mentioned previously, the velocity, *vel* in eqn (2.1) is limited within $vel_{\min} \le vel \le vel_{\max}$. These boundaries determine the resolution, with which regions are searched between the present position and target position. If the range of *vel* is too high, particles may search a large area, lacking the ability to converge. As the unknown variables are E and F (the real and imaginary part of the voltage, $V = E + jF$), it is therefore necessary to determine the limit of the velocity in terms of the voltage, V and angle, θ.

Table 4.11: Parameter sensitivity analysis of velocity limit for IEEE 30-bus system for normal load

(% × search space)	*Ave Iter*	*Ave Time*[s]	*S.R.* (%)	*Std Dev*	*H*		
					Best	*Average*	*Worst*
10%	5.30	0.11	100	1.15×10^{-6}	0	1.62×10^{-6}	5.0×10^{-6}
20%	6.70	0.13	100	1.48×10^{-6}	0	1.16×10^{-6}	7.0×10^{-6}
30%	19.3	0.35	64	1.06×10^{-6}	0	9.68×10^{-7}	4.0×10^{-6}
40%	15.1	0.28	48	9.67×10^{-7}	0	7.92×10^{-7}	5.0×10^{-6}
50%	12.3	0.23	18	8.02×10^{-7}	0	9.44×10^{-7}	3.0×10^{-6}
60%	12.3	0.23	32	2.73×10^{-6}	0	1.44×10^{-6}	1.5×10^{-5}
70%	9.50	0.18	41	1.24×10^{-6}	0	1.37×10^{-6}	4.0×10^{-6}
80%	10.1	0.19	41	1.16×10^{-6}	0	9.51×10^{-7}	4.0×10^{-6}
90%	12.4	0.23	36	9.31×10^{-7}	0	8.61×10^{-7}	3.0×10^{-6}
100%	9.10	0.18	42	9.68×10^{-7}	0	1.12×10^{-6}	4.0×10^{-6}

Table 4.12: Parameter sensitivity analysis of velocity limit for IEEE 30-bus system for 152.04% of normal load

% × search space	*Ave Iter*	*Ave Time*[s]	*S.R. (%)*	*Std Dev*	*H*		
					Best	*Average*	*Worst*
10%	8.3	0.15	100	1.05×10^{-6}	0	1.35×10^{-6}	5.0×10^{-6}
20%	8.02	0.15	96	1.20×10^{-6}	0	1.69×10^{-6}	6.0×10^{-6}
30%	9.3	0.17	94	1.27×10^{-6}	0	1.78×10^{-6}	6.0×10^{-6}
40%	8.9	0.16	71	1.63×10^{-6}	0	1.80×10^{-6}	8.0×10^{-6}
50%	10.3	0.19	69	1.67×10^{-6}	0	2.03×10^{-6}	9.0×10^{-6}
60%	9.0	0.17	62	1.37×10^{-6}	0	1.79×10^{-6}	5.0×10^{-6}
70%	10.1	0.19	70	1.90×10^{-6}	0	2.04×10^{-6}	1.3×10^{-5}
80%	10.8	0.20	73	1.95×10^{-6}	0	2.03×10^{-6}	1.0×10^{-5}
90%	10.1	0.18	61	1.10×10^{-6}	0	1.59×10^{-6}	5.0×10^{-6}
100%	10.8	0.20	65	1.25×10^{-6}	0	1.57×10^{-6}	6.0×10^{-6}

In this analysis, the velocity limit is set starting from 10% to 100% of search space with the step increment of 10% as shown in Table 4.11 and 4.12. Results in Tables 4.11 and 4.12 show success rate of 100% when the velocity limit is confined within 10% of the search space. Similarly, from the graph in Figure 4.10, setting the velocity limit to 10% of the search space is the best setting found in both cases of normal and heavy load. Hence, this setting will be applied to all future experiments from this point forward.

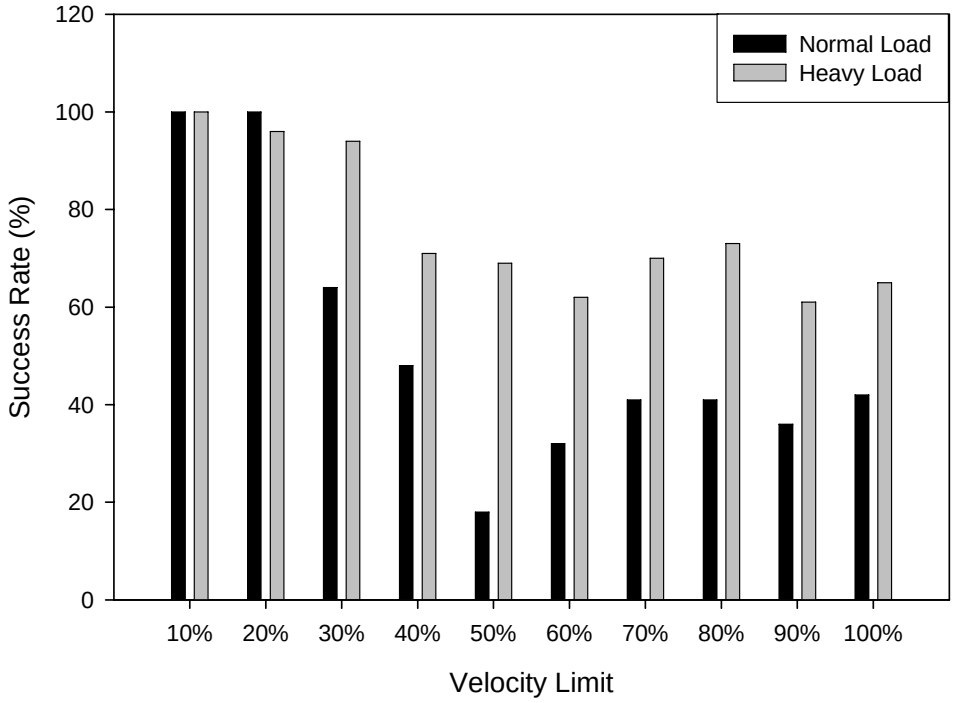

Figure 4.10: Success rate versus velocity limit for normal and heavy loads.

4.9 Conclusions

In this chapter, five experiments have been run to investigate the characteristics of the parameter settings in PSO. Through this preliminary analysis, a thorough understanding concerning the settings in PSO is acquired. As a conclusion, we propose a set of parameter settings (Table 4.13) to be applied in the future works using PSO algorithm.

Table 4.13: Proposed parameter settings for future works.

Parameter	Setting
Inertia weight, w	0.1 for any system
Population size, N	8 for IEEE 30-bus, 12 for IEEE 57-bus and 16 for IEEE 118-bus
Mutation probability, mp	0.4 for IEEE 30-bus and 57-bus 1.0 for IEEE 118-bus
r_1 , r_2	Uniformly distributed within [0, 1]
vel_{min}, vel_{max}	10% of search space

Chapter 5

5. Finding Maximum Loading Point (MLP) using Hybrid CGA/PSO Algorithm

5.1 Introduction

In validating the hybrid CGA/PSO algorithm for finding the load flow solution of power systems under the heavy load condition and to compare its performance with ACGA, the following test systems and load variations have been used:

1. IEEE 30-bus system with load increment from 52.86% to 53.09% of normal loading
2. IEEE 57-bus system with load increment from 40.78% to 40.86% of normal loading

3. IEEE 118-bus system with load increment from 61.37% to 61.40% of normal loading

The data specifications of the above power systems are downloadable from [104]. The optimal parameter settings found from the empirical study in chapter 3 are applied to the proposed hybrid method. Similar number of population size is applied to both algorithms for fair comparisons. In other words, the same parameter settings are applied. In an instant of load increment, different population sizes are applied. The common population sizes comprising of 50 and 100 individuals are applied. The success rate (S.R. (%)) is included for better clarification of reliability of the proposed method. For better comparison in terms of speed, both average iterations and time recorded are included. The load increment starts from the point whereby the proposed method start to obtain success rate less than 100%. As of such, the proposed method is still able to obtain 100% of success rate on 52.86%, 40.78% and 61.37% for the respective test systems.

5.2 Parameter Settings of PSO

In this thesis, the parameters ρ_1 and ρ_2 are set to constant values, which are commonly set as 2.0. The r_1 and r_2 are two random values, uniformly distributed in [0, 1]. The value of V_{max} in this thesis is 10% of the search range,

which is the best value from empirical study for the load flow problem (see Section 4.8 in Chapter 4). The common parameter settings for both algorithms are given in Table 5.1. Other parameters such as inertia weight (w) and population size (N) are found from the parameter sensitivity analysis presented in the previous chapter. These optimal settings are tabulated in Table 5.2.

Table 5.1: Common parameter settings for GA and Hybrid CGA/PSO

Parameter	Settings
Active and reactive power tolerance	0.001 p.u. on 100MVA base
Gradient acceleration, G	25% of the population
Number of trials	50
Maximum Generation, T	150
Initialisation range	$0.9 < V < 1.2$ and $-30° < \theta < 0°$
Population size, N	8 for IEEE 30-bus, 12 for IEEE 57-bus and 16 for IEEE 118-bus

Table 5.2: Parameter settings for relevant algorithms

Parameter	ACGA	Hybrid CGA/PSO
Crossover rate	Two-point crossover	Two-point crossover
Selection strategy	Roulette Wheel	Roulette Wheel
Mutation, *mp*	Uniform mutation with *mp* = 0.01	PSO mutation with *mp* = 0.4 for IEEE 30-bus and 57-bus, *mp* = 1.0 for IEEE 118-bus
Inertia weight, *w*	-	0.1
Maximum Velocity, V_{max}	-	10% of search space

5.3 Results

Results from the simulation are presented in Tables 5.3-5.5. For the IEEE 30-bus system, it is observed from Tables 5.3a and 5.3b that the hybrid CGA/PSO has a much higher success rate for finding the load flow solution when compared to ACGA for all the load increment points from 52.86% to 53.09%. For instance, the success rate of the hybrid CGA/PSO for the 52.86%, 52.89 and 52.92% load increment points are very close to 100%. The respective success rates recorded by the ACGA method are not satisfactory. The higher success rate obtained by the hybrid CGA/PSO signifies that the new algorithm has a much better performance than ACGA. Further more, the ACGA can no longer find anymore solutions beyond 53.04% load increment. However, the hybrid CGA/PSO can still find solutions with success rates within 52% to 18%, even under a small

population size of 8, just before the 53.09% load increment point, after which point there are no more feasible solutions. From the comparison of the execution times listed in Table 5.3a, it can be observed that the hybrid CGA/PSO is much faster than ACGA. The voltage profiles of IEEE 30-bus system for 52.86% and 53.09% load increments are shown in Table 5.6. All the PV nodes, as highlighted in Table 5.6 are converted to PQ nodes when the reactive power limits are reached.

Table 5.3a: IEEE 30-bus system (50 trials)

Load Inc (%)		52.86			52.89			52.92			52.95			52.98		
Population size		8	50	100	8	50	100	8	50	100	8	50	100	8	50	100
ACGA	S.R (%)	28	86	94	26	52	100	12	40	76	6	30	57	2	26	42
	Ave Iter	48	27	32	118	48	52	141	65	46	67	52	47	78	35	45
	Time[s]	0.41	2.4	3.7	0.8	4.0	9.2	1.0	5.2	8.9	0.6	4.0	7.9	0.7	4.9	8.4
Hybrid CGA/PSO	S.R (%)	100	100	100	90	92	100	96	98	100	88	98	100	86	94	100
	Ave Iter	26	24	22	49	52	35	32	43	30	45	37	31	43	38	35
	Time[s]	0.28	2.1	3.2	0.65	4.3	7.6	0.36	4.1	7.4	0.53	3.9	7.5	0.52	4.1	7.3

Table 5.3b: IEEE 30-bus system (50 trials)

Load Inc (%)		53.01			53.04			53.07			53.09		
Population size		8	50	100	8	50	100	8	50	100	8	50	100
ACGA	S.R (%)	0	16	20	0	0	4	0	0	0	0	0	0
	Ave Iter	-	92	68	-	-	94	-	-	-	-	-	-
	Time[s]	-	12.7	17.6	-	-	21.1	-	-	-	-	-	-
Hybrid CGA/PSO	S.R (%)	52	84	94	42	56	67	18	26	30	4	2	6
	Ave Iter	54	83	62	64	115	96	73	62	56	79	125	3
	Time[s]	0.6	9.2	15.6	0.7	10.9	17.5	0.8	7.5	13.2	0.9	16.7	23.4

For the case of IEEE 57-bus system, from the results in Tables 5.4a and 5.4b, similar conclusions as that for the case of the 30-bus system can be derived. For the case of IEEE 118-bus system; from Table 5.5, it can be observed that at the loading point of 61.37% load increment, the proposed hybrid CGA/PSO algorithm obtained the solution with 100% success rate despite the small population size of 16. On the other hand, the ACGA algorithm found the solution for the same loading point with a much lower success rate of 56%. For further load increment up to 61.40%, ACGA failed to find the solution but the proposed hybrid algorithm can still find the solution although the success rate is low. This indicates the proposed algorithm is much more powerful than ACGA. There are no more solutions present beyond the loading point of 61.40% of load increment. The voltage profile of the 54 generator nodes of the 118-bus test system at 61.37% load increment are tabulated in Table 5.7. The variation of voltage with

active power from normal load to 61.37% load increment for node 118 is illustrated in Figure 5.1.

Table 5.4a: IEEE 57-bus system (50 trials)

Load Inc (%)		40.78			40.79			40.80			40.81			40.82		
Population size		12	50	100	12	50	100	12	50	100	12	50	100	12	50	100
ACGA	S.R (%)	92	98	100	60	64	100	68	76	100	18	36	68	0	24	36
	Ave Iter	6	5	5	36	6	5	46	6	6	79	24	19	-	24	17
	Time[s]	0.75	2.8	5.5	1.5	4.7	8.6	2.8	3.1	5.9	4.1	7.1	18.2	-	6.8	11.3
Hybrid CGA/PSO	S.R (%)	100	100	100	90	88	100	76	82	100	32	72	80	24	48	50
	Ave Iter	6	5	5	15	7	6	20	8	8	42	16	23	33	18	23
	Time[s]	0.6	2.5	5.3	1.1	2.9	5.7	1.5	3.3	6.5	3.4	5.8	12.1	2.1	6.2	12.3

Table 5.4b: IEEE 57-bus system (50 trials)

Load Inc (%)		40.83			40.84			40.85			40.86		
Population size		12	50	100	12	50	100	12	50	100	12	50	100
ACGA	S.R (%)	0	0	12	0	0	8	0	0	4	0	0	0
	Ave Iter	-	-	43	-	-	37	-	-	51	-	-	-
	Time[s]	-	-	22.3	-	-	20.1	-	-	26.3	-	-	-
Hybrid CGA/PSO	S.R (%)	16	32	46	6	20	34	2	12	23	0	4	8
	Ave Iter	36	23	21	36	35	29	52	40	45	-	48	39
	Time[s]	2.3	6.7	11.2	2.2	8.2	13.6	3.1	9.8	21.2	-	11.7	19.6

For all the test cases from Table 5.3 to Table 5.5, the effect of increasing the population sizes in the proposed hybrid CGA/PSO algorithm is that the computing time is also increased. However, the number of iterations taken by the

algorithm does not necessarily increased when the population size becomes larger. This is due to the reason that a larger population size fastens the convergence, thereby resulting in less number of iteration.

Table 5.5: IEEE 118-bus system (50 trials)

Load Inc (%)		61.37			61.38			61.39			61.40		
Population size		16	50	100	16	50	100	16	50	100	16	50	100
ACGA	S.R (%)	56	72	100	48	54	76	32	26	54	0	0	0
	Ave Iter	11	7	7	12	8	7	14	9	7	-	-	-
	Time[s]	16.4	39.1	74.4	17.4	43.5	85.4	19.3	42.7	87.2	-	-	-
Hybrid	S.R (%)	100	100	100	92	90	100	48	72	96	0	2	6
CGA/PSO	Ave Iter	7.1	7.0	7.1	7.6	7.2	7.1	8.9	7.2	7.0	-	15.6	15.1
	Time[s]	9.6	30.9	64.7	10.3	31.4	62.5	10.7	32.4	63.3	-	131.5	256.1

Table 5.6: Voltage profile for IEEE 30-bus system

Load	52.86% load increment		53.09% load increment	
Node Index	Magnitude	Phase Angle (°)	Magnitude	Phase Angle (°)
1	1.060000	0.000000	1.060000	0.000000
2	**0.902526**	**-9.163226**	**0.898054**	**-9.193436**
3	0.825449	-14.144292	0.818886	-14.224428
4	0.779957	-17.714087	0.772084	-17.843672
5	**0.744227**	**-30.230791**	**0.735514**	**-30.673100**
6	0.746917	-21.817823	0.737926	-22.027609
7	0.726796	-26.740196	0.717579	-27.084412
8	**0.734867**	**-23.712009**	**0.725587**	**-23.968462**
9	0.737971	-30.984142	0.726524	-31.451153
10	0.699372	-36.278351	0.686610	-36.930237
11	**0.800427**	**-30.968399**	**0.789912**	**-31.432629**
12	0.743886	-34.378109	0.732089	-34.962929
13	**0.786679**	**-34.370037**	**0.775517**	**-34.952236**
14	0.706474	-37.226383	0.693927	-37.909386
15	0.692698	-37.416431	0.679860	-38.100208
16	0.708628	-36.032516	0.696212	-36.673157
17	0.689950	-36.905891	0.677058	-37.581543
18	0.665953	-39.475880	0.652561	-40.231888
19	0.657619	-40.039063	0.644044	-40.821728
20	0.666093	-39.276268	0.652661	-40.027641
21	0.669230	-37.823486	0.655811	-38.533367
22	0.670242	-37.767101	0.656822	-38.473484
23	0.661392	-38.628609	0.647855	-39.358040
24	0.639610	-39.044552	0.625182	-39.806389
25	0.641373	-38.172943	0.626557	-38.930454
26	0.596671	-39.874516	0.580452	-40.735943
27	0.664258	-36.653721	0.650009	-37.369335
28	0.727160	-23.398275	0.717403	-23.637709
29	0.609867	-41.403164	0.593751	-42.335968
30	0.578284	-45.204037	0.561152	-46.372238

Table 5.7: Voltage profile of generators' node for IEEE 118-bus system with 60% load increment

Node	V	θ°	Node	V	θ°	Node	V	θ°
1	0.9201	-90.71	42	0.9850	-67.05	80	0.9509	-9.34
4	0.9980	-83.19	46	0.8335	-26.93	85	0.9331	-23.75
6	0.9769	-86.70	49	0.9072	-31.80	87	1.0150	-26.65
8	1.0150	-74.78	54	0.9436	-45.63	89	1.0050	-18.87
10	1.0500	-59.95	55	0.9297	-45.79	90	0.9850	-26.79
12	0.9628	-87.62	56	0.9315	-45.53	91	0.9800	-26.17
15	0.9142	-83.50	59	0.9548	-35.98	92	0.9645	-24.20
18	0.9236	-82.87	61	0.9950	-26.19	99	1.0039	-25.44
19	0.9035	-83.00	62	0.9842	-26.99	100	0.9642	-28.50
24	0.9920	-56.04	65	0.9322	-12.12	103	0.9446	-35.71
25	1.0500	-59.90	66	0.9947	-18.58	104	0.9209	-40.62
26	1.0150	-58.61	69	1.0350	30.00	105	0.9235	-42.69
27	0.9680	-77.72	70	0.7631	-9.56	107	0.9520	-47.84
31	0.9670	-81.76	72	0.9436	-39.89	110	0.9549	-47.32
32	0.9607	-77.73	73	0.8623	-17.15	111	0.9800	-45.96
34	0.8673	-72.40	74	0.7117	-8.64	112	0.9750	-51.62
36	0.8610	-73.32	76	0.7069	-13.14	113	0.9930	-80.09
40	0.9700	-74.72	77	0.8628	-7.51	116	1.0050	-1.87

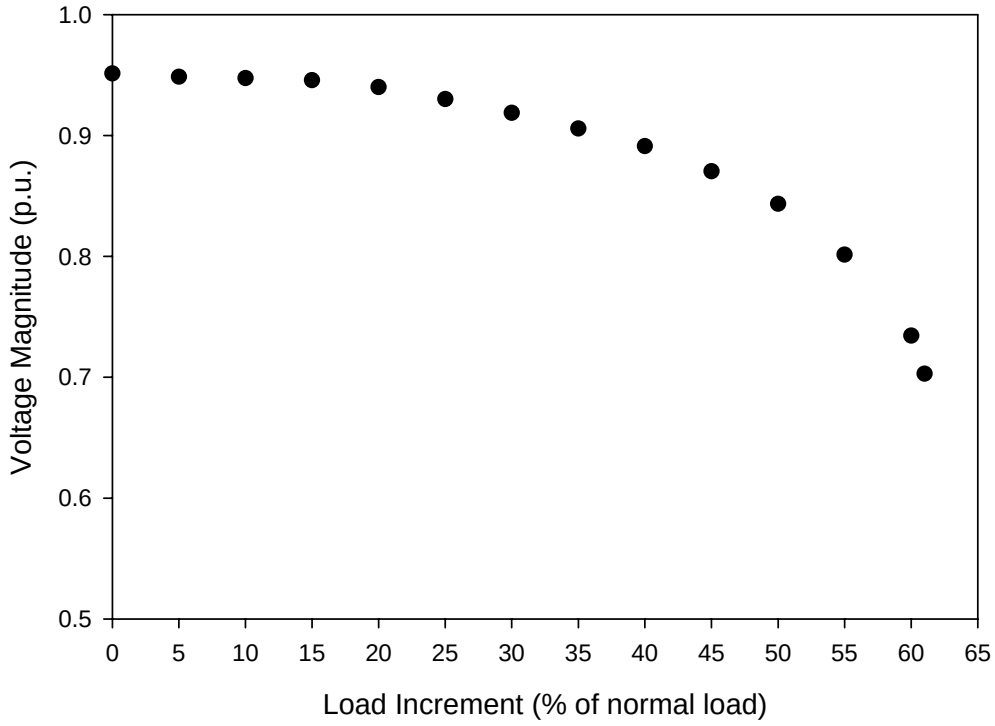

Figure 5.1: Variation of nodal voltage magnitude with load demand increment at node number 118

5.4 Results Comparison

Taking the maximum loading points (MLP) of the test systems to be the highest loading points found by the ACGA and the proposed hybrid algorithm with 100% success rate, the MLPs of the test systems found are tabulated in Table 5.8. The MLPs found the hybrid CGA/PSO are higher than those by ACGA especially those for the 118-bus test system. The improvement is due to the replacement of the nodal voltage differential acceleration technique in ACGA by PSO in forming the hybrid CGA/PSO algorithm.

Table 5.8: Comparison of Maximum Loading Point (MLP)

System	MLP (% of Load Increment)	
	ACGA	Hybrid CGA/PSO
IEEE 30-bus	52.23	52.86
IEEE 57-bus	40.70	40.78
IEEE 118-bus	60.70	61.37

5.5 Conclusions

The hybrid CGA/PSO load flow algorithm developed in Chapter 3 has been applied to three IEEE test systems. The hybrid algorithm has been found to be much more powerful and efficient than the previous ACGA algorithm particularly when it is applied to evaluate the load flow solution of heavy-loaded power systems. The large capability of the proposed algorithm allows it to evaluate the maximum loading points with better accuracy for larger systems than ACGA.

Chapter 6

6. Locating Type-1 Load Flow Solutions via Hybrid CGA/PSO Load Flow Algorithm

6.1 Introduction

With the increasing load demand and exploitation of power transmission system, problems related to voltage instability have been receiving continuous interest in research. Since 1970s, voltage instability has been the root cause of several power systems collapses worldwide [87, 88]. The voltage stability problem has now become a source of concern in highly developed and mature networks as a result of heavier loadings and power transfers over long distances. Consequently, voltage stability is increasingly being addressed in system planning and operating studies.

Although the work in [14, 23, 24] is able to locate all the load flow solutions, the connection of these solutions in regards to voltage stability remains to be indistinct. Type-1 solution simply means that the corresponding

Jacobian matrix of the load flow solution set has exactly one eigenvalue with a positive real part and the rest of the eigenvalues have negative real parts. In general, a solution is considered Type-*k* when there are *k* positive values for the real part of the eigenvalues whereby these eigenvalues can be either complex number or real number. In other words, Type-1 solutions have only one eigenvalue with a positive real part while Type-2 solution has two positive real part values.

Works presented in [27, 28] link the Type-1 solutions to the voltage stability assessment by stating that only Type-1 load flow solutions are closely associated with voltage instability phenomenon. Based on this fact, the computational cost can be further reduced by locating only the Type-1 load flow solutions while the other solutions are not a major concern for stability assessment. Recently, works in [27, 28] present different strategies in locating Type-1 load flow solutions. However, the method in [27] lacks in the ability in locating all the possible Type-1 solutions present in a large system while the performance of CPFLOW-based algorithm in [28] is unknown for large system as only small systems are adopted for test problems.

A graphical illustration showing the contribution of hybrid GA/PSO in the searching process is shown in the right hand side of Figure 6.1 while the left hand side figure illustrates the condition of search dependent solely on gradient information. It can be observed that the hybrid GA/PSO plays a crucial role as

a local search, optimizing the solution space in each generation.

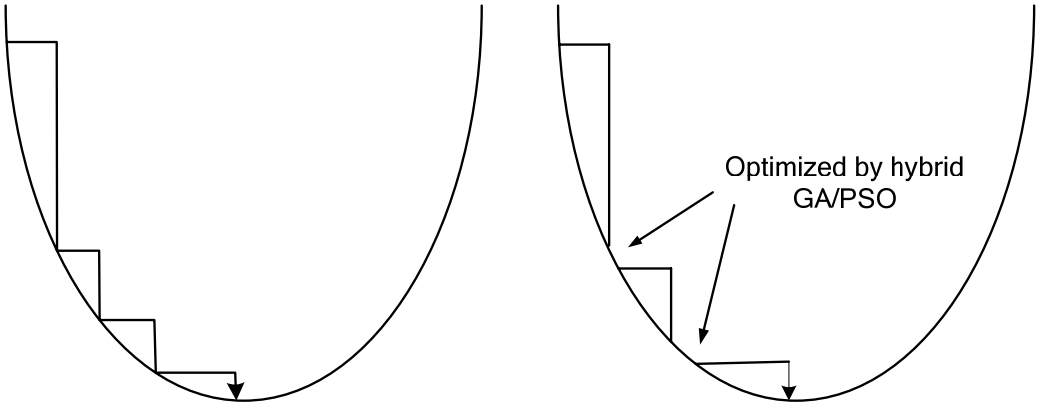

Figure 6.1: Graphical illustration of search process

In this chapter, a technique based on the Hybrid Genetic Algorithm / Particle Swarm Optimisation is used to find the Type-1 load flow solutions. The following sections in this chapter are organised as follows. The experimental settings are available in Section 6.2 with results presented in Section 6.3. Discussion on characteristics of Type-1 solutions is in Section 6.4 and finally the conclusions are derived in Section 6.5.

6.2 Experiment Settings

Two test systems [23, 24, 14, 91] are adopted to demonstrate the robustness of the proposed hybrid algorithm. The network data with specified generation, loads and nodal voltages for both systems are given in Figures 6.2

and 5.3. Under these conditions, the 5-bus system has 10 load flow solutions while the 7-bus system has 5 load flow solutions.

The parameter settings adopted in this experiment is summarised in Table 6.1. A population size comprises of 20 candidates is initialised within the specified range given in Table 6.2. The maximum number of iterations is set to 100 and number of trials to be carried out is 50 times. Some parameters such as crossover rate, gradient acceleration, PSO mutation rate and inertia weight are optimal settings found from previous study in [92]. As the initialisation range is crucial in our study here, different sets of initialisation ranges are proposed for further investigation, shown in Table 6.2.

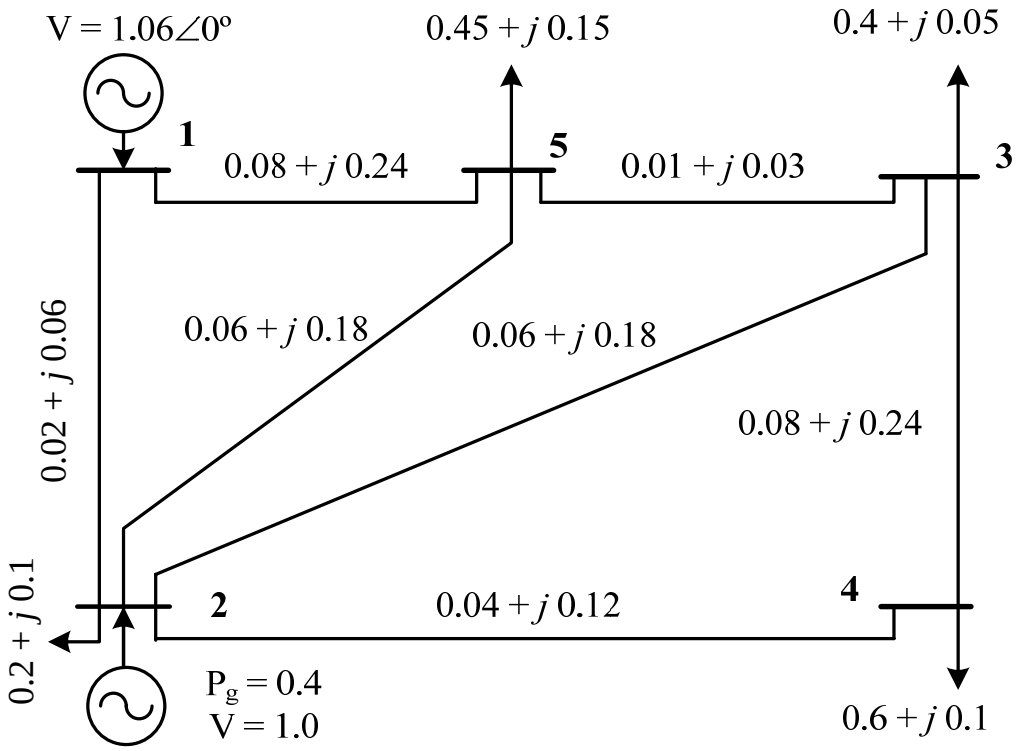

Figure 6.2: The 5-bus system

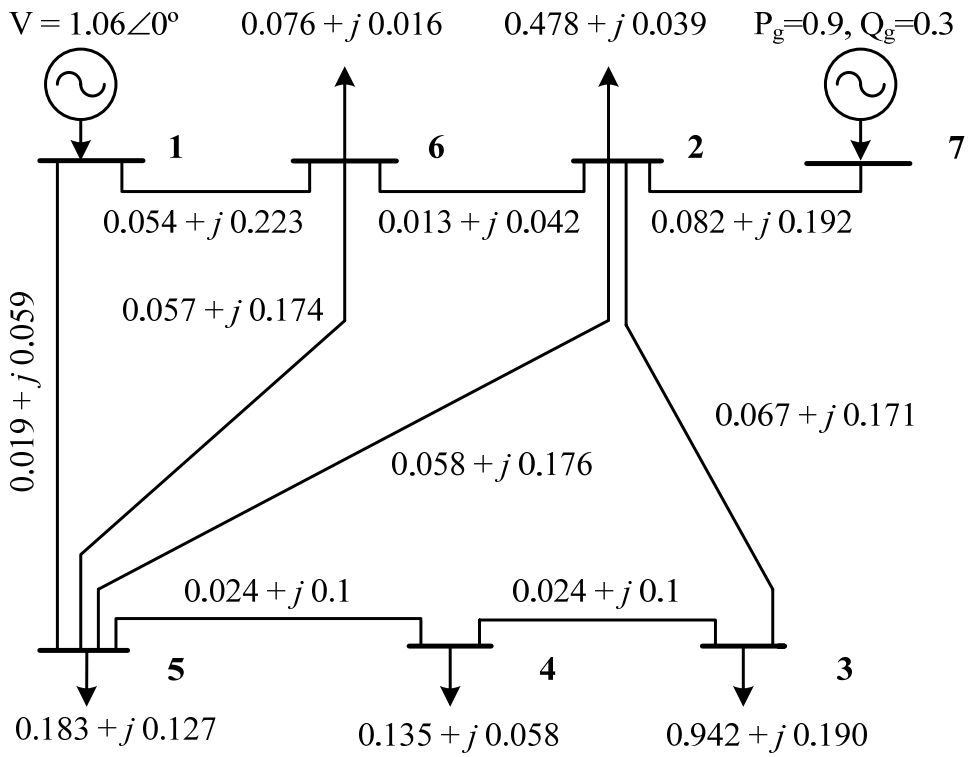

Figure 6.3: The 7-bus system

Table 6.1: Common parameter setting for all experiments

Parameter	Setting
PQ tolerance	0.001 p.u. on a 100MVA base
Population size	20
Maximum Generation	100
Number of trials	50
Initialisation range	Given in Table 6.2
Gradient acceleration	25% of the population
Crossover	2-point crossover with probability 0.9
Selection strategy	Roulette wheel
PSO mutation rate	0.04
Inertia weight	0.1 is appropriate for any load

Table 6.2: Initialisation range

Set	Voltage (p.u.)	Angle (º)
A	0.0-0.5	-180º to -90º
B	0.0-0.5	-90º to 0º
C	0.0-0.5	-180º to 0º
D	0.5-1.0	-180º to -90º
E	0.5-1.0	-90º to 0º
F	0.5-1.0	-180º to 0º
G	0.0-1.0	-180º to 0º

In Table 6.2, the initialisation ranges *A*, *B* and *C* have low voltage profile whereas sets *D*, *E* and *F* have high voltage profile ranges. All the angles for *A*-*E* have an angle range of 90° except for sets *F* and *G* which have an angle range of 180°. On the other hand, the voltage range is 0.5 p.u. except for set *G*, having voltage range of 1.0 p.u. Statistical information from the experiment, with the success rate is given in Tables 6.3 and 6.4.

6.3 Results

Results depicted in Tables 6.3 and 6.4 show the frequency of solution of the specific load flow solution obtained by the algorithm. In Table 6.3, the number from 1 to 10 at the first row represents the 10 load flow solutions present in the 5-bus system. As 7-bus system has 4 solutions, therefore number from 1 to 4 is available in the first row of Table 6.4. Using the range set as

specified in Table 6.2, the hybrid GA/PSO is run and frequency of each solution is calculated. For example, in Table 6.3, out of 50 runs using set *B*, there are eight solutions number 6, one solution number 7, sixteen solutions number 8 and seventeen solutions number 9. Thereby, the success rate calculated is 46/50=0.92. The solutions, showing the voltage profile for both systems are given in Tables 6.5 and 6.6.

Each initialisation set results in different coverage of the multiple load flow solutions. From careful analysis with respect to initialisation range, it is found that the solutions obtained usually located within the initialisation range or nearby. For example, for set *A* in Table 6.3, 27 solutions are solution number 10. From the details of the node voltages available in Table 6.5, it is examined that solution number 10 has low voltage profile and large negative angles for *PQ* and *PV* nodes. Therefore, initializing the voltages and angles within 0.0 and 0.5 p.u. assists in a smoother convergence. In terms of the success rate, the 5-bus system records an overall success rate of 0.91. This success rate deteriorates when applied to 7-bus system with overall success rate recorded as 0.67. This implies the degree of difficulty due to three reasons. Firstly, 7-bus system involves a greater number of nodes and therefore more variables are present which increases the complexity of the final solution. Secondly, by observing the normal load solution (solution number 1) as depicted in Table 6.6, node 3 records a voltage of 0.904 p.u. which implies that the load at

this node is heavier than usual. In general, light load nodes usually operate with a voltage close to unity value. Thirdly, the design of the initialisation range in Table 6.2 is not optimal for this system. From the analysis of angles in Table 6.6, there is actually no common range for these angles.

Table 6.3: Frequency of multiple solutions for 5-bus system (50 runs)

Set	Solution Number										Success rate
	1	*2	3	*4	5	*6	7	*8	9	10	
A	0	0	3	0	15	0	0	0	1	27	46/50=0.92
B	0	0	0	0	0	8	1	16	17	0	42/50=0.84
C	0	0	3	0	9	4	1	7	7	7	38/50=0.76
D	0	48	1	0	1	0	0	0	0	0	50/50=1.00
E	32	0	2	4	4	5	0	3	0	0	48/50=0.96
F	3	7	1	0	7	19	6	7	0	0	50/50=1.00
G	0	1	2	0	7	14	1	13	5	2	45/50=0.90
Total	35	56	12	4	43	48	9	46	30	36	319/350=0.91

* Type-1 solutions

Table 6.4: Frequency of multiple solutions for 7-bus system (50 runs)

Set	Solution Number				Success rate
	1	*2	*3	4	
A	0	0	1	29	30/50=0.60
B	0	0	0	36	36/50=0.72
C	0	1	0	28	29/50=0.58
D	0	1	1	15	17/50=0.34
E	1	19	0	28	48/50=0.96
F	0	5	1	29	35/50=0.70
G	0	2	0	38	40/50=0.80
Total	1	28	3	203	235/350=0.67

* Type-1 solutions

Table 6.5: The ten solutions of the 5-bus power system (Type-1 solutions are identified by *)

No	Solutions				
	$V_1 \angle \theta_5°$	$V_2 \angle \theta_1°$	$V_3 \angle \theta_3°$	$V_4 \angle \theta_4°$	$V_5 \angle \theta_2°$
1	1.060 ∠ 0.000	1.000 ∠ -2.067	0.977 ∠ -4.853	0.966 ∠ -5.692	0.980 ∠ -4.535
*2	1.060 ∠ 0.000	1.000 ∠ -138.967	0.587 ∠ -134.863	0.831 ∠ -141.660	0.501 ∠ -129.851
3	1.060 ∠ 0.000	1.000 ∠ -128.586	0.410 ∠ -124.173	0.066 ∠ -185.734	0.377 ∠ -116.836
*4	1.060 ∠ 0.000	1.000 ∠ -12.146	0.740 ∠ -13.879	0.057 ∠ -71.501	0.793 ∠ -12.679
5	1.060 ∠ 0.000	1.000 ∠ -126.625	0.215 ∠ -144.796	0.698 ∠ -133.440	0.062 ∠ -159.529
*6	1.060 ∠ 0.000	1.000 ∠ -16.504	0.030 ∠ -81.865	0.628 ∠ -23.451	0.197 ∠ -26.042
7	1.060 ∠ 0.000	1.000 ∠ -18.097	0.049 ∠ -80.670	0.632 ∠ -25.443	0.056 ∠ -61.126
*8	1.060 ∠ 0.000	1.000 ∠ -16.908	0.184 ∠ -37.786	0.686 ∠ -23.872	0.034 ∠ -69.046
9	1.060 ∠ 0.000	1.000 ∠ -22.520	0.036 ∠ -85.945	0.081 ∠ -79.418	0.196 ∠ -30.681
10	1.060 ∠ 0.000	1.000 ∠ -119.882	0.165 ∠ -144.756	0.075 ∠ -178.499	0.088 ∠ -141.839

Table 6.6: The four solutions of the 7-bus power system (Type-1 solutions are identified by *)

No	Solutions						
	$V_1 \angle \theta_1°$	$V_2 \angle \theta_2°$	$V_3 \angle \theta_3°$	$V_4 \angle \theta_4°$	$V_5 \angle \theta_5°$	$V_6 \angle \theta_6°$	$V_7 \angle \theta_7°$
1	1.0 ∠ 0.0	0.964 ∠ -2.934	0.904 ∠ -8.444	0.928 ∠ -5.750	0.964 ∠ -2.446	0.968 ∠ -2.592	1.076 ∠ 5.2860
*2	1.0 ∠ 0.0	0.588 ∠ -5.221	0.175 ∠ -52.678	0.412 ∠ -14.206	0.723 ∠ -3.206	0.664 ∠ -4.303	0.731 ∠ 14.958
*3	1.0 ∠ 0.0	0.542 ∠ -6.293	0.543 ∠ -19.810	0.646 ∠ -11.246	0.775 ∠ -3.862	0.640 ∠ -5.016	0.288 ∠ 101.819
4	1.0 ∠ 0.0	0.433 ∠ -6.835	0.250 ∠ -44.280	0.436 ∠ -16.136	0.688 ∠ -3.919	0.550 ∠ -5.314	0.344 ∠ 88.336

For instance, the solution number 4 records an angle of 88.336° for node 7 which is very far from the angle in node 3, recorded as -44.280°. Hence, redesign of the initialisation set will ultimately produce better results for this

7-bus system. Despite lacking the convergence capability, all the multiple solutions (including Type-1 solutions) present in both systems are found.

Among 10 solutions in 5-bus system, there are four Type-1 solutions present whereas for 7-bus system, only two Type-1 solutions are present. These values are denoted with asterisk (*) at the left side of solution number in Tables 6.3 and 6.4. Again, the voltage profile of the Type-1 solutions can be found in Tables 6.5 and 6.6 whereby they agree to the results presented in [28]. The eigenvalues recorded are available in Table 6.7 which are discussed in the next section.

6.4 Characteristics of Type-1 Solutions

Type-1 load flow solutions have been previously known as low-voltage solutions [28]. Type-1 solutions consist of the following characteristics:

6.4.1 One Positive Value for Real Part of Eigenvalues

As mentioned in the previous section, there exists only one eigenvalue with positive real-part among total eigenvalues present in a system. The eigenvalues of the Jacobian matrix for both test systems are available in Table 6.7. The set of eigenvalues for Type-1 can consist of purely real or complex numbers. However, no purely imaginary eigenvalues are possible as Type-1 solution is located at hyperbolic equilibrium point.

Table 6.7: Eigenvalues of Jacobian matrix For Type-1 solutions

5-Bus System				7-Bus System	
*2	*4	*6	*8	*2	*3
7.97	-20.92	-40.5-13.4i	-21.49	-21.7-6.8i	-23.2-6.8i
-20.7-6.9i	3.8-0.6i	-40.5+13.4i	-4.7-0.9i	-21.7+6.8i	-23.2+6.8i
-20.7+6.9i	-3.8+0.6i	-23.78	-4.7+0.9i	-19.5-5.8i	-19.3-6.0i
-9.0-2.6i	-1.4-0.2i	-4.48-0.74i	**0.45**	-19.5+5.8i	-19.3+6.0i
-9.0+2.6i	-1.4+0.2i	-4.48+0.74i	-0.45	-4.8-1.6i	-8.6-2.1i
-3.1-0.6i	-0.39	-0.62	-1.2-0.1i	-4.8+1.6i	-8.6+2.1i
-3.1+0.6i	**0.38**	**0.57**	-1.2+0.1i	**0.71**	-4.3-1.4i
				-2.8-0.7i	-4.3+1.4i
				-2.8+0.7i	**0.67**
				-1.84	-1.68
				-0.93	-1.18
				-1.16	-0.71

6.4.2 Nodal Voltage Level of Type-1 Solutions

Type-1 solutions often have one node with the lowest voltage for the relevant node among the multiple solutions. However, this does not apply to all the Type-1 solutions obtained. Table 6.8 depicts the voltages for all the nodes in 5-bus system from the results obtained. The total solutions obtained are 10 and among these, solutions 2, 4, 6 and 8 are Type-1 solutions. These are being highlighted by an asterisk in the relevant table. From these Type-1 solutions, only solution number 4, 6 and 8 depicts the characteristic mentioned. For instance, the voltage of node 3 in solution number 6 recorded a voltage of

0.030 p.u. which is the lowest voltage in the row. Similarly, this characteristic is also shown in solutions number 4 and 8.

Table 6.8: Voltages of 5-bus power system (10 solutions)

	1	2*	3	4*	5	6*	7	8*	9	10
V_1	1.060	1.060	1.060	1.060	1.060	1.060	1.060	1.060	1.060	1.060
V_2	1.000	1.000	1.000	1.000	1.000	1.000	1.000	1.000	1.000	1.000
V_3	0.977	0.587	0.410	0.740	0.215	**0.030**	0.049	0.184	0.036	0.165
V_4	0.966	0.831	0.066	**0.057**	0.698	0.628	0.632	0.686	0.081	0.075
V_5	0.980	0.501	0.377	0.793	0.062	0.197	0.056	**0.034**	0.196	0.088

6.4.3 Coalesce with Normal Solution at Bifurcation

This characteristic is illustrated in Figure. 6.4, whereby 5-bus system is adopted in this case. This system has 10 solutions at normal load, 5 solutions at (100%× normal load) load increment, 4 solutions at (200%×normal load) load increment, 2 solutions at (300%×normal load) load increment. Type-1 solution is guaranteed to exist in any load condition. As the system loading is varied, the locations of these solutions also vary. The number of solutions decreases until (385%×normal load) load increment, only normal solution and a single Type-1 solution remain.

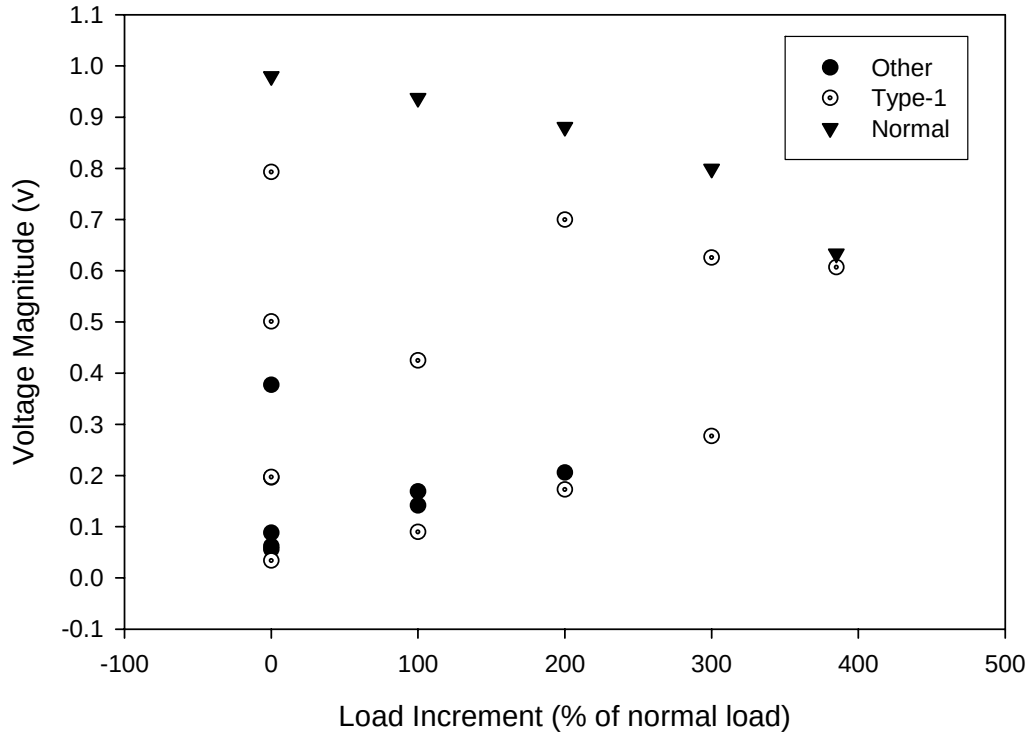

Figure 6.4: PV curve at node 5 of 5-bus system

At this point, the two solutions is said to coalesce on the maximum loadability boundary (denoted by ∑) in a saddle-node bifurcation. This condition is shown in Figure 6.4. On the other hand, analysis on 7-bus system found that the system encounters the maximum loadability boundary when the increment is (94%×normal load).

6.5 Conclusions

It has been shown that the hybrid GA/PSO is capable of locating all the load flow solutions for the two test systems. No solution curves tracing is required in the proposed method. In addition, the hybrid GA/PSO is able to

find a pair of solutions consisting of normal and Type-1 solutions at the vicinity of the bifurcation point. The characteristics of the Type-1 solutions have been investigated and their characteristics presented. The proposed methodology is promising for use in finding the Type-1 solutions for voltage stability assessment purposes.

Chapter 7

7. Calculation of Power System Security Margins and Contingency Analyses via Fast Infeasible Method (FIM)

7.1 Introduction

Security Margins in the context of power system refers to availability of generated power to keep the system secure from voltage collapse in the case of contingencies due to either generator outage or branch outage, so as to maintain the stability of power system operation. In power system analysis, maintaining load flow solvability is of great importance. When unsolvable cases occur in contingency analysis, no further analysis can be done for recovery. Additionally, in terms of voltage stability, restoring load flow solution has a great importance. After a severe power outage, the systems experience

reduction of load demand and the loads tend to recover to normal load level state as shown in Figure 7.1. The new load level state will determine the stability of the system. In steady state analysis, the system will be stable whenever the Maximum Loading Point (MLP) is beyond the normal load, specified as λ_0=1.0 in Figure 7.1. On the other hand, voltage collapse occurs when the MLP for the relevant contingency is less than 1.0. At this point, the system is not able to reach a stable equilibrium state. Thus, the security margin as being illustrated in Figure 7.1 is the available power margin from normal load up to the MLP (λ^{MLP}) of the system.

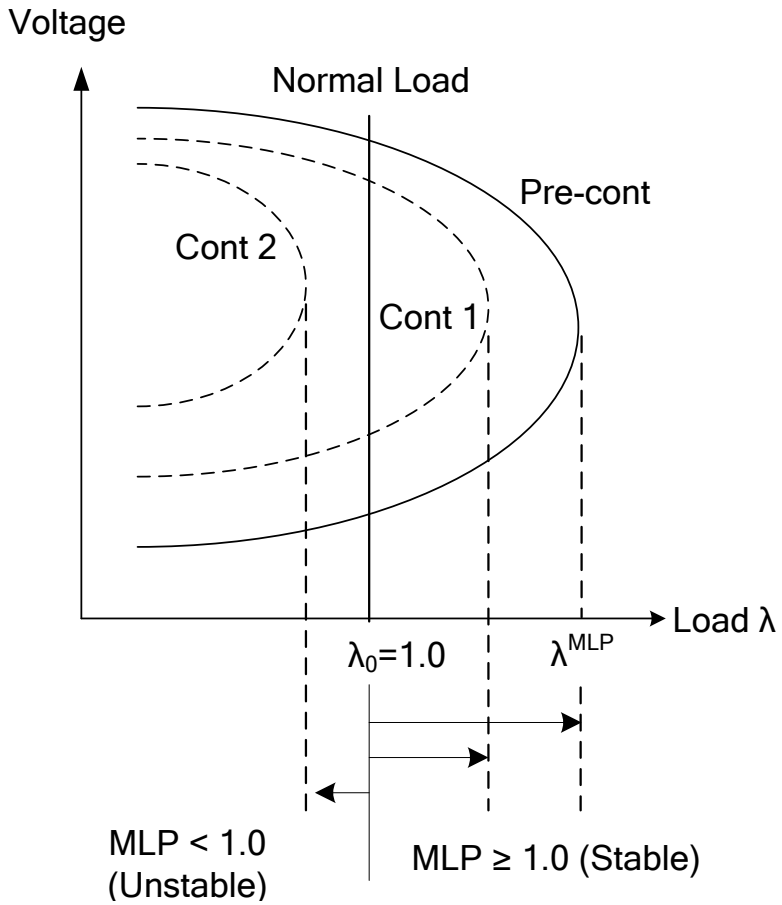

Figure 7.1: Maximum Loading Point (MLP) change due to contingencies

Massive systems interconnections, increasing power demand, economical and environmental reasons have enforced a demand for power companies to operate their equipments very close to the limit of the system. Therefore, it is necessary to evaluate the system's operating conditions with respect to voltage stability under both normal and heavy loaded scenarios. The evaluation done for short-term and long-term analyses has the outcome leading to expansion planning, operation planning and real time operation. Over the previous decades numerous techniques have been developed to determine the voltage stability limits. These methods can be categorised into different classes:

i. Bifurcation analysis [93]-[97]
ii. Investigating the type of load flow solution [24, 25, 28, 99, 101].
iii. Finding Maximum Loading Point (MLP) of system [31, 32, 35, 36, 102, 103]

This chapter focuses on a new approach to find MLP when (a) the system is operating normally, (b) branch outage occurs and (c) generator breaks down. In order to verify that a power system has reached the loadability limit, different way of checking can be employed. Works in [33, 34] utilise the Jacobian matrix minimum singular value as the indication of stability limit. Similarly, the MLP is estimated in [35] by using a set of stable operating point which is

based on the analysis of Jacobian matrix behaviour. Some general sensitivity formulas at saddle-node bifurcation (SNB) have been derived in [107], stating the four properties that must be satisfied at SNB. The presence of a pair of multiple solutions can also be checked using techniques proposed in [25] to determine the maximum loading condition. This approach is implemented in this thesis as the previous work in [99] has proven that the proposed hybrid algorithm is capable of locating the pair of solution at bifurcation point.

Most methodologies mentioned are solely to find the MLP values when the system is at a stable state and does not demonstrate the capability of performing contingency analysis due to branch and generator outage. There have been various studies concerning branch outage contingencies. However, the voltage stability evaluation (finding MLP values) for generator outage is a new topic, which is proposed recently by N. Yorino in [53]. The analyses of MLP during contingency are also included in this thesis. Methods proposed in [94, 95] utilise and manipulate the Jacobian matrix obtained without recalculation of the load flow solution to find bifurcation point of a system. As of such, even when the load flow is recalculated, the solution may not converge if the solution lies near to the steady state limit of a system due to highly nonlinear condition at this stage. This limitation does not present in the proposed method as the hybrid CGA/PSO [92] is adopted to solve the load flow problem in each step towards the MLP of a system. In general, vigorous research has been carried

out in computing the MLP for different conditions and system characteristics. Though efficient, most of them do not provide the actual or accurate figure stating the limit of the system due to the highly nonlinear characteristics present near the MLP of a system. Therefore, the search for refined solutions still deserves special attention.

The solution strategy proposed here starts from the infeasible region whereby no solution can be found. The loading factor λ is decreased in every iteration. The size of the decrement is determined by a mathematical proven formulation adopted from [31, 32]. Only a few iterations (less than 10) are required to determine the MPL of a system. Thus, this method is named as Fast Infeasible Method (FIM). With respect to this approach, more accurate MPL values are achieved in this thesis with appropriate computational cost using a simple approach. Furthermore, some contingency analyses are presented demonstrating the capability of the proposed method to find MLP in regards to branch and generator outage. The effectiveness of the proposed method is demonstrated through the IEEE 14-, 30- and 57-bus systems.

The organisation of the remaining part in this chapter is as follows. Section 7.2 outlines the load flow problem and explains the formulation of infeasible recovery equation. The proposed methodology is described in Section 7.3 while the application studies with test results are presented in section 7.4. Numerical results comparison with the existing method is done in

the same section. Further analysis considering branch outage is carried out in Section 7.5 with results comparison in Section 7.6. Finally, the conclusions and recommendations are derived in Section 7.7.

7.2 Problem Specifications

7.2.1 Load Flow Problem

The load flow equations can be written in terms of the state variables $\boldsymbol{x}$ and parameter λ as

$$\boldsymbol{g}(\boldsymbol{x}, \lambda) = 0 \tag{7.1}$$

λ is referred to as the system-loading factor, set to a value larger than 1 ($\lambda > 1$). With λ set to 1, means the normal load conditions are applied. Eqn. (7.1) above can also be explained by the following mathematical term

$$\begin{aligned} &\sum_{i=1}^{n}\left(\lambda P_i^{sp} - P_i^c\right) = 0, \quad i \in \{PQ,\ PV\,buses\} \\ &\sum_{i=1}^{n}\left(\lambda Q_i^{sp} - Q_i^c\right) = 0, \quad i \in \{PQ\ buses\} \end{aligned} \tag{7.2}$$

where P_i^{sp} and Q_i^{sp} are the specified active and reactive powers at any node *i* whereas P_i^c and Q_i^c are the calculated active and reactive powers at any bus *i*. The calculated active power (P_i^c) and reactive power (Q_i^c) at bus *i* are given by:

$$\begin{aligned} P_i^c &= E_i \sum_{j=1}^{n}(G_{ij}E_j - B_{ij}F_j) + F_i \sum_{j=1}^{n}(G_{ij}F_j + B_{ij}E_j) \\ Q_i^c &= F_i \sum_{j=1}^{n}(G_{ij}E_j - B_{ij}F_j) - E_i \sum_{j=1}^{n}(G_{ij}F_j + B_{ij}E_j) \end{aligned} \tag{7.3}$$

Considering a power system which in unusual case has a load present in a *PV* bus, therefore P_i^{sp} and Q_i^{sp} can be view as the net power that can be comprehended as:

$$\begin{aligned} P_i^{sp} &= P_i^G - P_i^L \\ Q_i^{sp} &= Q_i^G - Q_i^L \end{aligned} \tag{7.4}$$

whereby P_i^G and Q_i^G are powers from generator at bus i whereas P_i^L and Q_i^L are the load demand at bus i. From eqns. (7.2) and (7.4), it is important to notice that with (λ>1), not only increases the load demand but also increases the generated powers. This has been claimed in [32] to be the usual way to define load increase in voltage stability analyses which is also employed in this thesis. The same way is being carried out in [31, 32] and in real world application in [100]. Hence, similar methodology is adopted in this thesis. From eqn. (7.2), the same loading factor λ for both active and reactive powers implies that the load varies with constant power factor, followed by a proportional real power generation variation. Also, limits on reactive power generation capacities are considered. In case a *PV* bus violates its reactive power generation limit, the relevant bus is converted to *PQ* bus. The possibility of this *PQ* bus to return to its original *PV* bus is also taken into account in the available program.

7.2.2 Infeasible Recovery Formulation

The expression of updating the loading factor, λ^{t+1} is adopted from [31, 32] whereby the superscript t+1 represents the next iteration. The idea here is to

formulate a way to bounce the load flow solution back to feasible region from infeasible region. The mathematical equation for this expression is given as

$$\lambda^{t+1} = \lambda^{t} - \left(\sum_{i=1}^{n} \left(\Delta P_i^2 + \Delta Q_i^2 \right) \right)^{1/2} \tag{7.5}$$

which can be further simplified to

$$\lambda^{t+1} = \lambda^{t} - Err \tag{7.6}$$

whereby *Err* is the square root of the total mismatches of active and reactive powers. The expression of load update above is very simple, being computed basically with the power mismatches calculated and specified powers. From the simulation results in the next section, the update based on eqn. (7.6) proves to be efficient in pulling the system onto the feasibility boundary.

7.3 Proposed methodology – Fast Infeasible Method (FIM)

7.3.1 Solving the Load Flow problem

The load flow problem has been described in Section 3.2. In regards to MLP, the Continuation Power Flow (CPF) in [36] has been the most popular method which is shown to be effective even for solutions close to collapse boundary. However, instead of adopting the CPF, the hybrid CGA/PSO developed in the previous work in [92] is applied as the core mechanism in this thesis. Despite the non-deterministic feature of the hybrid CGA/PSO, it is able to cope better with the nonlinear load models. Results presented in [92] prove the capability of the algorithm to find an operable solution in the vicinity of bifurcation point

with high reliability and appropriate computational time. The parameter settings adopted in this experiment is summarised in Table 7.1. A population size comprises of 20 candidates is initialised within the specified range given in the same table. The maximum number of iterations is set to 50 and the number of trials to be performed is 20 times. Some parameters such as crossover rate, gradient acceleration, PSO mutation rate and inertia weight are optimal settings found from parameter sensitivity analysis.

Table 7.1: Parameter settings

Parameter	Setting
PQ tolerance	0.001 p.u. on a 100MVA base
Population size	8
Maximum Generation	50
Number of trials	20
Initialisation range	$0.7 < V < 0.8$ and $-40° < \theta < -20°$
Gradient acceleration	25% of the population
Crossover	2-point crossover with probability 0.9
Selection strategy	Roulette wheel
PSO mutation rate	0.4
Inertia weight	0.1

7.3.2 Tackling MLP from infeasible region

In this thesis, the MLP is found starting from infeasible operating region. This

simply means that a value of λ which is assumed to be located at the infeasible region is set on the first iteration. The initial value, λ^0 is set to 2.0 and this value is employed to all the test systems. This strategy of tackling the MLP from infeasible regions eliminates the complex formulation of calculating λ^{n+1} from the normal loading factor, λ=1.0 such as done in [32]. The location of λ in the solution space is illustrated in Figure 7.2 below whereby 4 iterations are required to approach MLP which is present at the nose point of the PV curve. From Figure 7.2, the search begins from the loading factor set to 2.0 (λ^0 = 2.0). Through the update via eqn. (7.6), the load adjustment size ($\Delta\lambda = \lambda^t - \lambda^{t-1}$) decreases and reach λ^{MLP} in four load flow iterations.

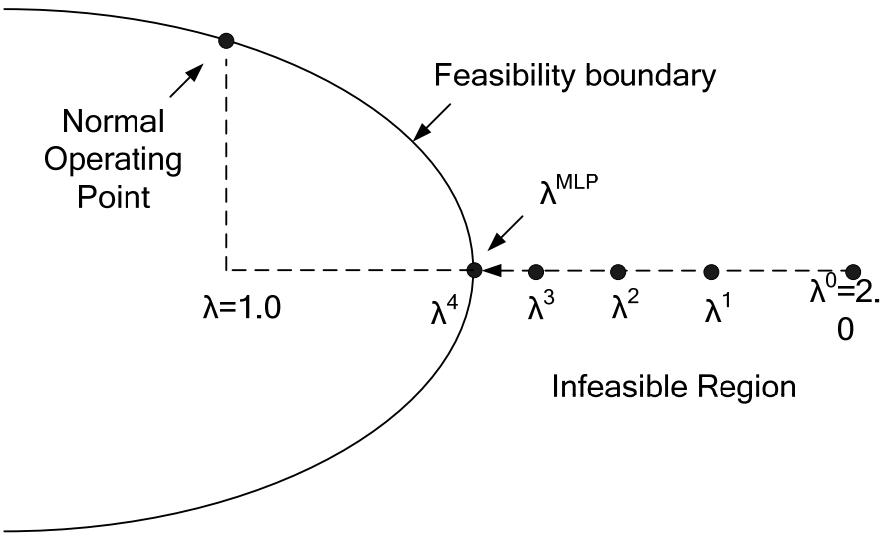

Figure 7.2: Approach to MLP from infeasible region

From our preliminary simulation, it has been found that the update of loading factor based on eqn. (7.6) is able to locate the MLP values for IEEE 14-,

30- and 57-bus systems using the initial value of loading factor λ^0=2.0. The update based on eqn (7.6) might not be efficient if λ^0 is far away from λ^{MLP}. This is because when λ^0 is far from λ^{MLP}, the value of mismatches, *Err* becomes large. This results in a large adjustment for λ and at times even negative values. To avoid this abnormal update, only the load flow solution with high fitness is chosen for the update in eqn. (7.6). Figures 7.3-7.5 depict the fitness of the load flow solution at λ=2.0 versus *Err*. Each dot in these graphs represents a trial. Therefore, each graph consists of 50 dots as each test system is run for 50 trials. From these graphs the total violations for IEEE 14- and 30-bus is no more than 1.2. This maximum violation increases up to around 22 for IEEE 57-bus. This indicates the importance of choosing the right load flow solution for the update of λ. In this methodology the best solution out of 5 load flow trials is chosen for the update of λ specified in eqn. (7.6), illustrated in Figure 7.6. Using this strategy it can be assured that the total violations of *P* and *Q* is small.

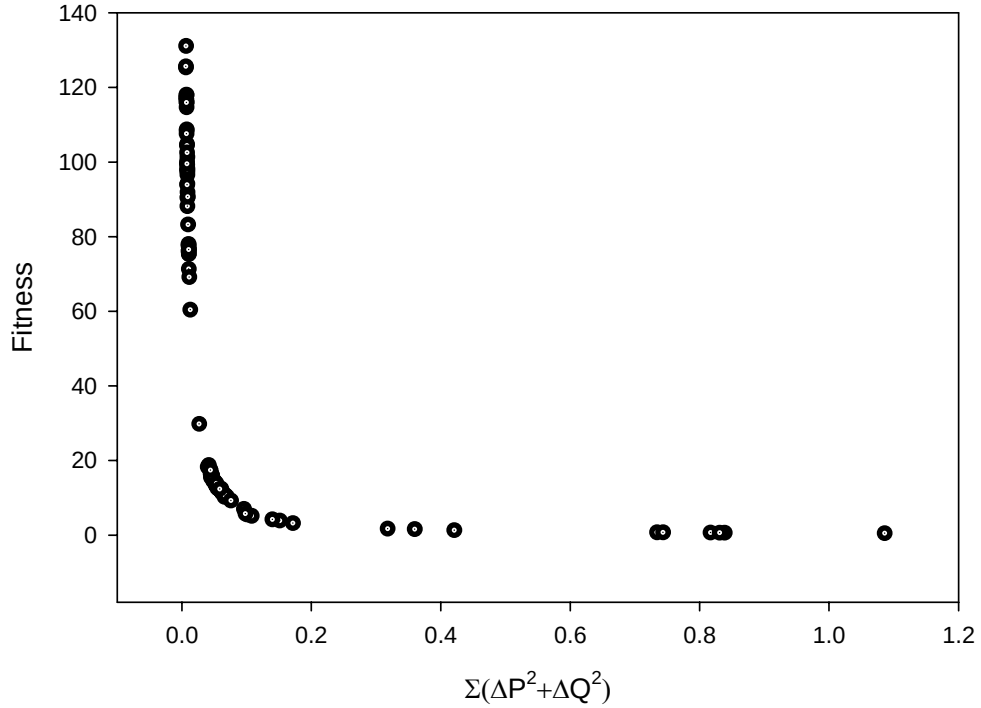

Figure 7.3: Fitness of best solution for IEEE 14-bus system at λ=2.0 for 50 trials

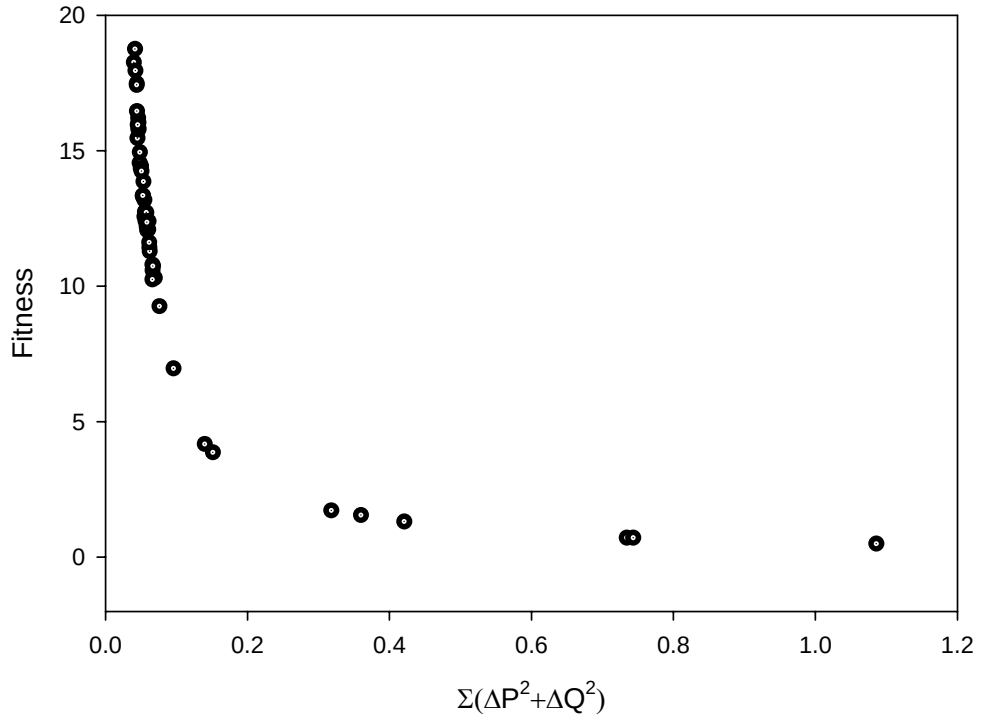

Figure 7.4: Fitness of best solution for IEEE 30-bus system at λ=2.0 for 50 trials

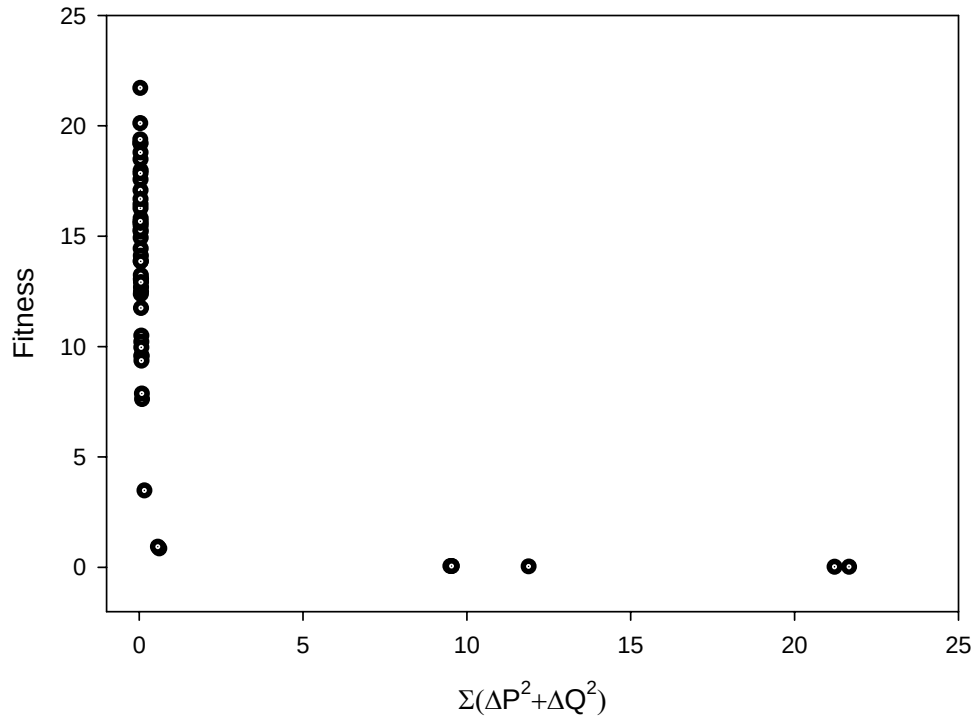

Figure 7.5: Fitness of best solution for IEEE 57-bus system at λ=2.0 for 50 trials

The flow of FIM is illustrated by a flow chart in Figure 7.6. This figure depicts a very simple flow of FIM, which is able to find the maximum loading point λ^{MLP} within few updates of loading factor λ. Results shown in section 7.4 verify this efficiency. From Figure 7.6, an initial loading factor λ^0 is set to 2.0. Then the hybrid CGA/PSO is applied to solve the load flow within 3 trials. The failure of the load flow means that the loading factor is infeasible. Therefore, it is necessary to decrease the loading factor using eqn. (7.6). This update will continue until the load flow solution is found. It is important to note that hybrid CGA/PSO is capable of finding multiple solutions. Therefore, all the non-operable (Type-1, Type-2, Type-3 etc.) solutions are eliminated by

using the similar method as done in the previous work presented in [99]. This is carried out by calculating the eigenvalues of the load flow's Jacobian matrix. In general, a solution is considered Type-*k* when there are *k* positive values for the real part of the eigenvalues whereby these eigenvalues can be either complex number or real number.

The entire flow in Figure 7.6 represents one run/trial. In the proposed method, 20 trials are run and the best, average and worst are recorded, presented in Table 7.2 in Section 7.4. Two factors facilitate the encouraging results. The first factor is contributed by effective solution of load flow even in the vicinity of bifurcation point. The second factor is the fast and accurate update of loading factor λ using eqn. (7.6). Hence, the FIM can be applied to find the maximum loading point in any system automatically and accurately.

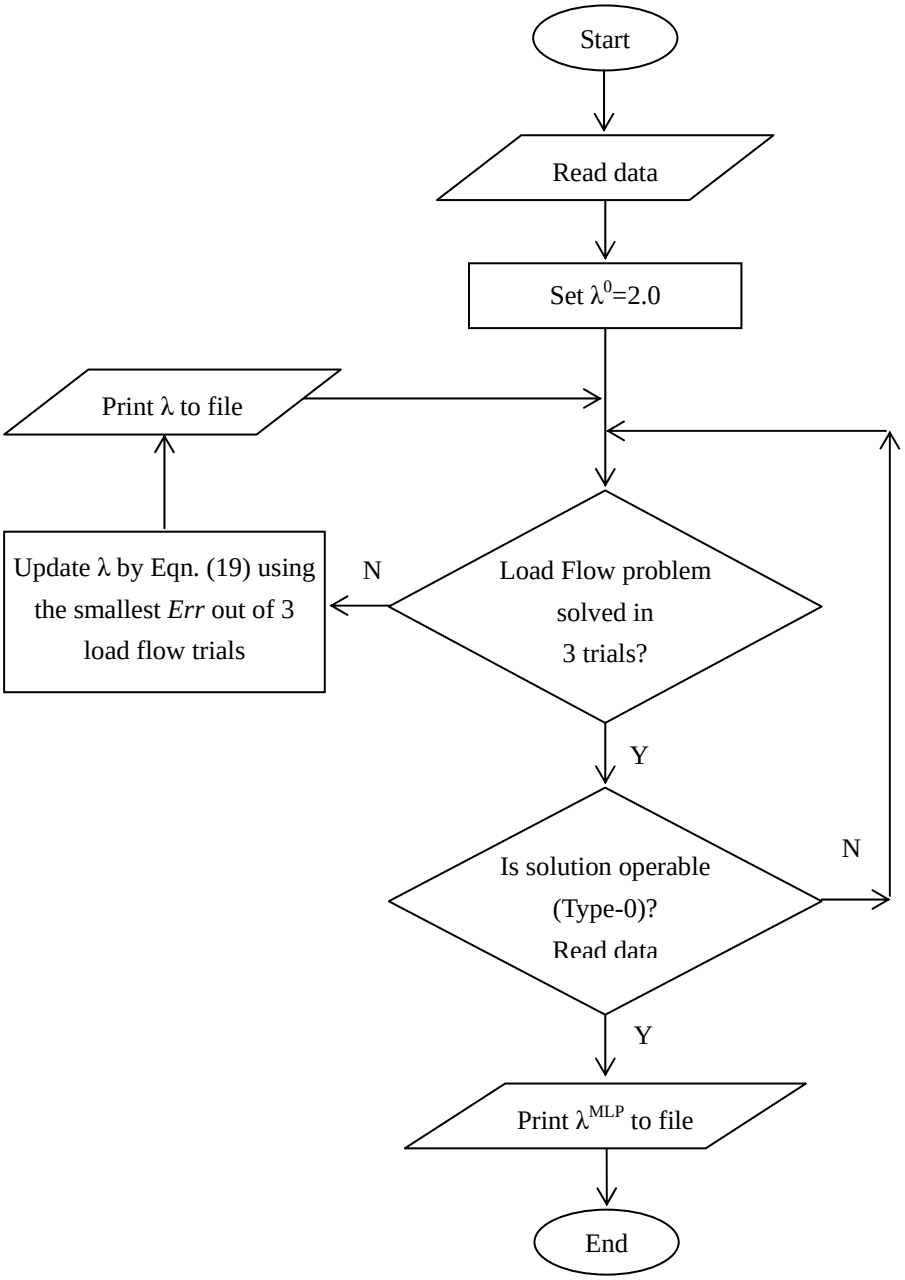

Figure 7.6: Flow of Fast Infeasible Method (FIM)

7.4 Application Studies

The proposed method has been tested and evaluated for commonly used power systems test suite. In this section, test results for IEEE test systems are presented and discussed. The proposed method is applied to three IEEE test

systems available from [104]. Results from simulation are divided into two parts. The first part is given in Section 7.4.1 below, which presents the evolution of loading factor λ with respect to the load flow iterations. This is followed by numerical values of λ^{MLP} obtained, discussed in Section 7.4.2. Further, the results comparison with some existing methods portrays the superiority of the proposed method in finding the MLP value of a system.

7.4.1 Evolution of Loading Factor λ

The update and evolution of the loading factor λ for all test systems are illustrated in Figures 7.7-7.9. The λ^{MLP} obtained are given in each of the figures. From these graphs, the proposed strategy is effective in finding λ^{MLP} as only 5 load flow iterations are required for convergence based on the evolution of λ on IEEE 14-bus system, as observed in Figure 7.7 whereby each dot represent one load flow iteration. Another two systems require 6 iterations as depicted in Figures 7.8 and 7.9. The average of λ update is recorded in Table 7.2. With the starting point from the infeasible region, hence avoiding the complex mathematical formulation to start from λ^0=1.0, which is not required in the proposed strategy.

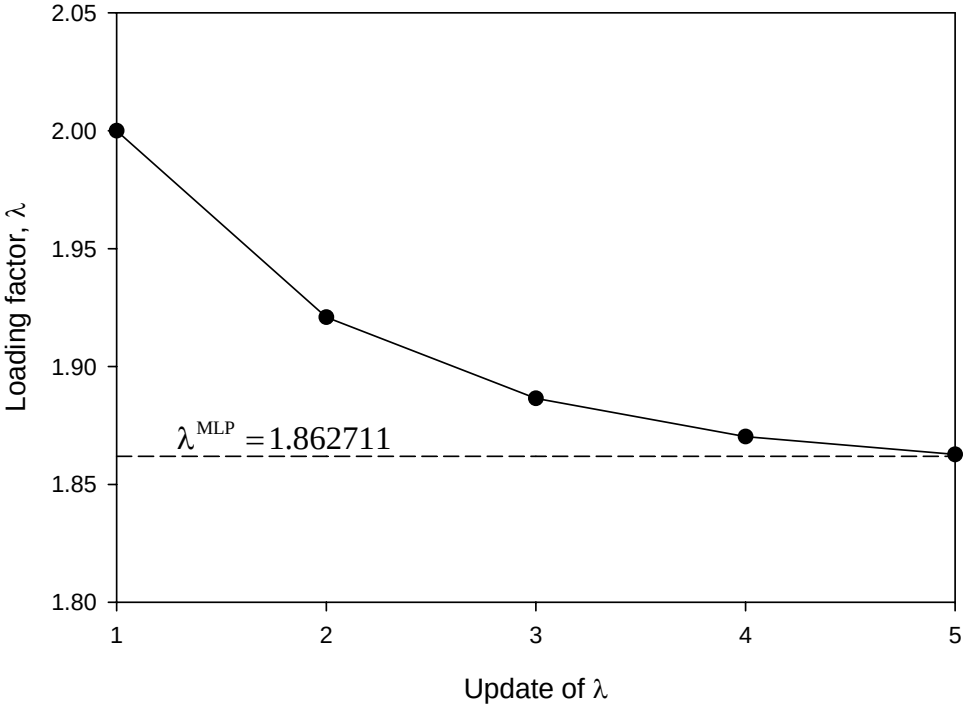

Figure 7.7: Evolution of λ on IEEE 14-bus system

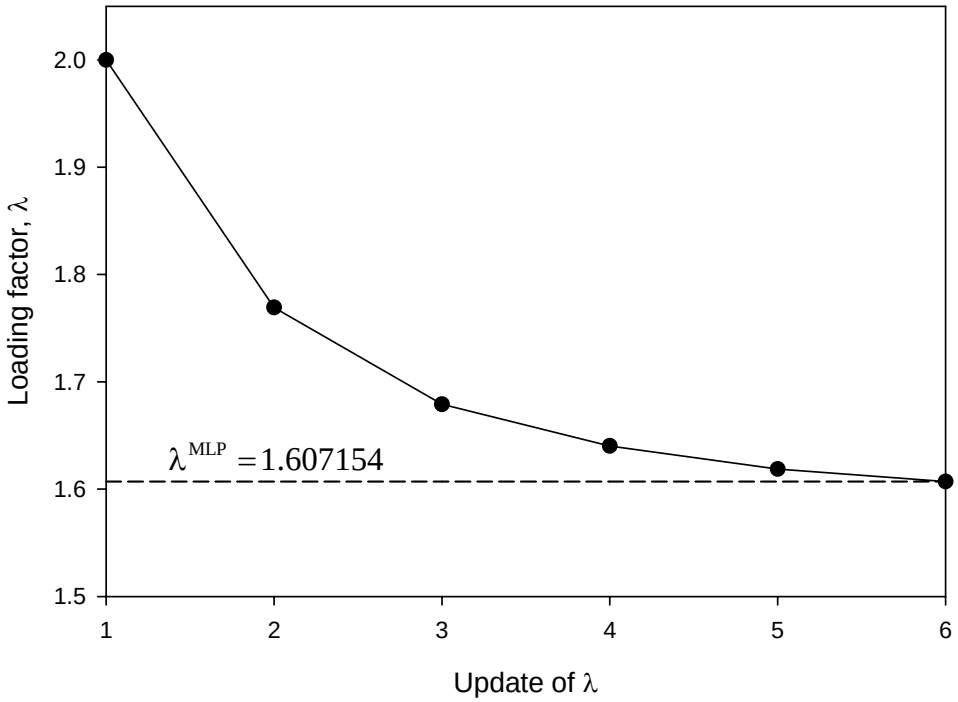

Figure 7.8: Evolution of λ on IEEE 30-bus system

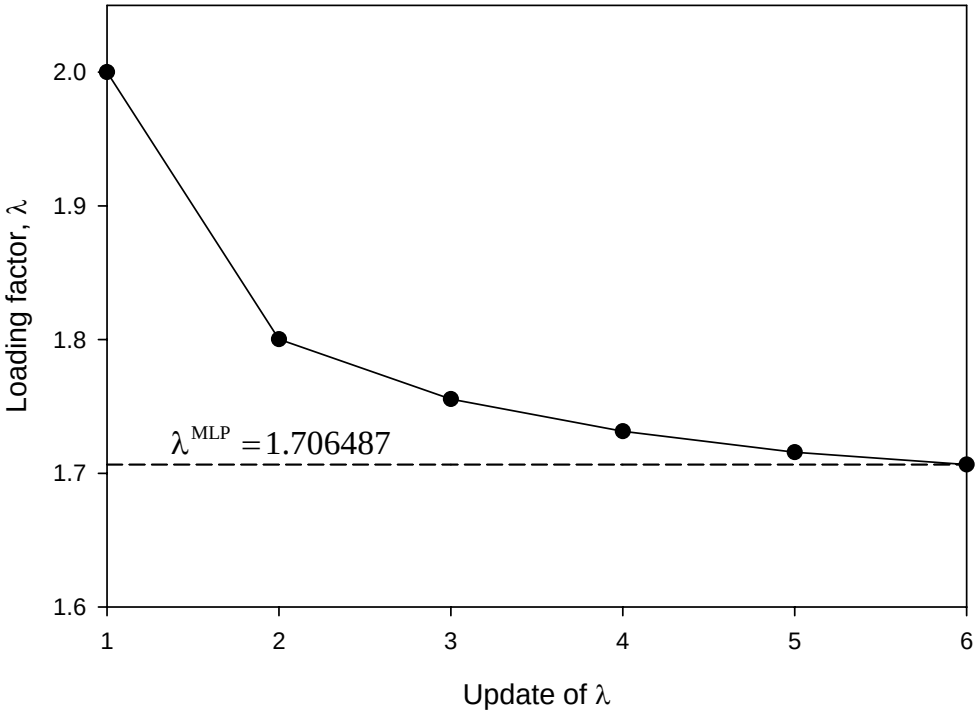

Figure 7.9: Evolution of λ on IEEE 57-bus system

7.4.2 Numerical Results and Comparisons

Results from the simulation for IEEE test systems are given in Table 7.2. The core focus in this table is the value of the maximum loading point λ^{MLP}. Hereby, from 20 trials, the best, average and worst results are recorded for further analysis. The initial starting point, λ^{0} is given in Table 7.2. As the proposed method is based on the stochastic method which is based upon the random exploration of the search space with intrinsic intelligence, therefore it is not possible to obtain deterministic results. However, when the difference of the best and worst is carefully examined, it can be concluded that only a slight difference is observed, which means that FIM is stable and reliable.

Table 7.2: Results of FIM on common test systems (20 trials)

System	λ^0	Std Dev	λ^{MLP}			Ave λ Update
			Best	Ave	Worst	
IEEE 14-bus	2.0	6.93×10^{-4}	1.86182	1.86089	1.85962	5
IEEE 30-bus	2.0	1.67×10^{-3}	1.60460	1.60189	1.59925	6
IEEE 57-bus	2.0	1.33×10^{-3}	1.70335	1.69654	1.64049	6

To show the advantage of the proposed method, results from very recent work [31, 32] is adopted for comparison in Table 7.3. The result of the well-known Continuation Power Flow (CPF) method is also included in the third column of the same table. The results of CPF are generated from the toolbox available in using the default settings in the toolbox except that the reactive power limit is included under the CPF settings. Results comparison depicted in Table 7.3 shows the advantage of the proposed method despite the non-deterministic feature of load flow solutions. In all the test cases, the value of λ^{MLP} shows greater loading factor values compared to other methods; thereby increasing the known security margins in voltage stability analysis. To ensure the feasibility of these limits, these values are manually set into the running program and results conclude that all the λ^{MLP} are feasible, thereby verified the validity of the increased MLP values of the test systems.

Table 7.3: Results comparison of λ^{MLP}

System	Nonlinear Prog [31]	LFSSO [32]	CPF	FIM
IEEE 14-node	1.8550	1.8550	1.7763	1.8618
IEEE 30-node	1.5934	1.5934	1.5290	1.6072
IEEE 57-node	1.6943	1.6943	1.6119	1.7033

7.5 Contingency Analyses

The linear sensitivity method [46, 47, 49] is a fast computation method and is useful in providing the direction for countermeasures, although the errors are large for quantitative margin calculations for severe contingencies. Work presented in [48] presents the calculation of load power margins for both branch and generator outage contingencies using linear and non-linear sensitivity methods. In this section, the proposed method is tested and shown to be capable of estimating either the pre-contingency or post-contingency voltage stability margin. Under either contingency condition, the voltage stability margin is related to system's load power margin to operate in stable condition. The load power margin is widely accepted as a most informative index representing directly the degree of voltage stability. The load power margins ΔP in p.u. is calculated by:

$$\Delta P = \left(\lambda^{MLP} - 1\right) \times P_0 \qquad (7.7)$$

where P_0 is the base loading at the operating point corresponding to λ_0=1.0 illustrated in Figure 7.1. Considering the IEEE test systems, the P_0 calculated for 14-, 30- and 57-bus are 2.59 p.u., 2.834 p.u. and 12.508 p.u. respectively.

A one line diagram of the IEEE 14-bus test system used here is given in Figure 7.10. It consists of 5 PV buses (five synchronous machines, including 3 synchronous compensators used only for reactive power support). There are 3 transformers, 20 branches and 14 buses with 11 loads totalling 259 MW and 81.4 MVar. A capacitor acting as shunt susceptance with a value of 0.19 p.u. is present at bus number 9, providing reactive power support. Besides IEEE 14-bus test system, other systems adopted as test bed in this thesis are IEEE 30- and 57- bus.

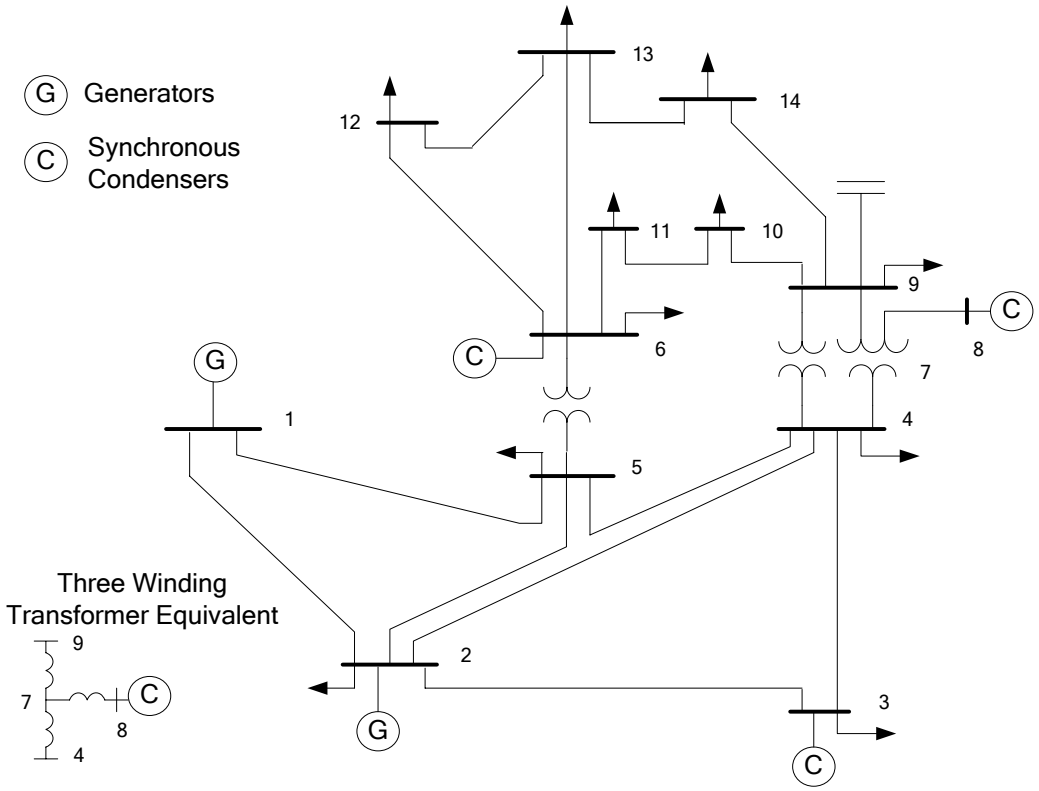

Figure 7.10: IEEE 14-bus test system

7.5.1 Branch Outage

Under the condition of branch outage contingency, all the possible branch outages are tested except for the cases where islanding occurs. To simulate branch outage contingency, the relevant i^{th} admittance is set to zero G_{ij}=B_{ij}=0.0. Then, the shunt admittances of the two ends of the outage branch are also set to zero $G_{ij}^{s} = B_{ij}^{s} = 0.0$. The graph showing the evolution of loading factor for relevant branch outage contingencies for IEEE 14-bus system is illustrated in Figure 7.11. Numerical results are presented in Tables 7.4, 7.5 and 7.6. The values of maximum loading point λ^{MLP} are recorded with the power margin calculated from eqn. (7.7). In addition, the stability state for each branch

outage is also recorded. From Figure 7.11, it is observed that the number of load flow iterations differs for different branch outages. It means that each branch outage poses a different level of complexity to the entire system. The largest number of iterations recorded is 7; during branch outage of line 7-9 whereas the least is 2 iterations only, in the case of branch outage of line 2-3. In all three test systems, only the first case causes the system to be unstable with $\lambda^{MLP} < 1.0$. The systems remain in stable state for other branch outage contingencies.

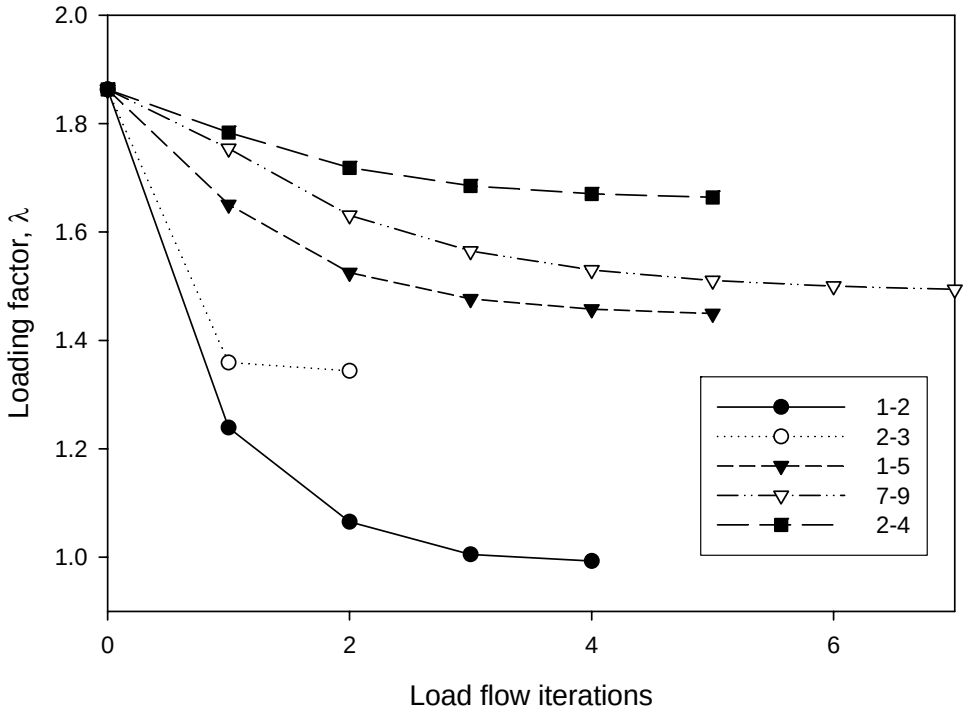

Figure 7.11: Relevant branch outage contingencies for IEEE 14-bus system

Table 7.4: Loading factor λ for branch outage contingencies for IEEE 14-bus system with base loading, P_0=2.59 p.u.

No.	Branch Outage	λ^{MLP}	Stability	ΔP [p.u.]
1	1-2	0.990297	Unstable	-0.02513
2	2-3	1.343601	Stable	0.889927
3	1-5	1.447587	Stable	1.159250
4	7-9	1.491786	Stable	1.273726
5	2-4	1.661321	Stable	1.712821

Table 7.5: Loading factor λ for branch outage contingencies for IEEE 30-bus system with base loading, P_0=2.834 p.u.

No.	Branch Outage	λ^{MLP}	Stability	ΔP [p.u.]
1	1-2	0.879701	Unstable	-0.340930
2	2-5	1.155412	Stable	0.440438
3	1-3	1.272721	Stable	0.772891
4	3-4	1.278962	Stable	0.790578
5	2-6	1.437953	Stable	1.241159

Table 7.6: Loading factor λ for branch outage contingencies for IEEE 57-bus system with base loading, P_0=12.508 p.u.

No.	Branch Outage	λ^{MLP}	Stability	ΔP [p.u.]
1	35-36	0.73253	Unstable	-3.3589
2	25-30	1.046845	Stable	0.5554
3	34-35	1.100339	Stable	1.2353
4	37-38	1.210110	Stable	2.6262
5	1-15	1.421565	Stable	5.2729

7.5.2 Generator outage

In general, the generator is operated with PV- or PQ-specified terminal condition. For a PV generator, the terminal voltage is regulated with AVR, while for a PQ generator the reactive power output is controlled as a constant. In this thesis, the PQ specified condition is assumed for all the generators that will be faulted. When a generator is faulted, the *P* and *Q* outputs become zero. In other words, the terminal condition must be switched from PV to PQ to simulate the generator outage condition. In this case, it is assumed that the emergency control is properly designed so that the loss in the active power is recovered by the incremental output of the other generators. This operation usually includes the active power balance between the generations and loads considering the response of speed governors of generators. All the possible generator outages are tested except the generator at the slack bus.

Results from the simulation are recorded in Tables 7.7-7.9. From the analysis of the stability of the system, there is only one generator outage that causes the system to collapse. This condition happens when generator 8 of IEEE 57-bus system breaks down. The power margins obtained from the update of loading factor λ based on eqn (7.6) are available in these tables.

Table 7.7: Loading factor λ for generator outage contingencies for IEEE 14-bus system, P_0=2.59 p.u.

No.	Generator	λ^{MLP}	Stability	ΔP [p.u.]
1	6	1.719264	Stable	1.8628
2	8	1.764647	Stable	1.9804
3	2	1.740815	Stable	1.9187
4	3	1.722468	Stable	1.8712

Table 7.8: Loading factor λ for generator outage contingencies for IEEE 30-bus system, P_0=2.834 p.u.

No.	Generator	λ^{MLP}	Stability	ΔP [p.u.]
1	8	1.466636	Stable	1.3224
2	5	1.496952	Stable	1.4084
3	2	1.511936	Stable	1.4508
4	13	1.523441	Stable	1.4834
5	11	1.531103	Stable	1.5051

Table 7.9: Loading factor λ for generator outage contingencies for IEEE 57-bus system, P_0=12.508 p.u.

No.	Generator	λ^{MLP}	Stability	Δ*P* [p.u.]
1	8	0.883144	Unstable	-1.4616
2	12	1.115737	Stable	1.4476
3	3	1.615103	Stable	7.6937
4	6	1.672068	Stable	8.4062
5	9	1.666738	Stable	8.3396
6	2	1.680649	Stable	8.5136

7.6 Results Comparisons

To evaluate the robustness of the proposed method, all the contingency cases are rerun using the Continuation Power Flow (CPF) method described in [36] with the toolbox available from [105]. The percentage of improvement is calculated from eqn. (7.8). The comments on the results and the calculated improvements are discussed in the relevant sub-sections below. The percentage of improvement is calculated based on the formula:

$$\text{Improvement (\%)} = \frac{P_{obtained} - P_{reference}}{P_{reference}} \times 100\% \qquad (7.8)$$

whereby $P_{obtained}=P_0 + \Delta P$, which is the obtained real power at the collapse point, P_0 is the base loading while $P_{reference}$ is the reference power obtained by either point of collapse (PC) or continuation power flow (CPF) method.

7.6.1 Branch Outage

The calculated power margins from CPF method for the branch outage cases are tabulated in Tables 7.10-7.12. In a glance, FIM is able to achieve considerable improvements for all the branch outage cases, with the largest improvement calculated as 12.30% for the branch outage of line 1-15 in IEEE 57-bus system. Most of the results from FIM are able to achieve 2%-4% improvement over the CPF method. This implies that FIM is capable of finding more accurate value

of power margins available during the branch outage contingency. Moreover, FIM does not encounter any convergence problem as in the case of CPF, whereby CPF is unable to converge to a solution for branch outage of line 35-36 for IEEE 57-bus system.

Table 7.10: Improvement of FIM over CPF for branch outage on IEEE 14-bus system with base loading, P_0=2.59 p.u.

No.	Branch Outage	FIM ΔP [p.u.]	CPF ΔP [p.u.]	Improvement (%)
1	1-2	-0.02513	-0.0672	1.67
2	2-3	0.889927	0.7780	3.32
3	1-5	1.159250	1.0277	3.64
4	7-9	1.273726	1.1523	3.24
5	2-4	1.712821	1.5379	4.24

Table 7.11: Improvement of FIM over CPF for branch outage on IEEE 30-bus system with base loading, P_0=2.834 p.u.

No.	Branch Outage	FIM ΔP [p.u.]	CPF ΔP [p.u.]	Improvement (%)
1	1-2	-0.340930	-0.3318	-
2	2-5	0.440438	0.3667	2.30
3	1-3	0.772891	0.6578	3.30
4	3-4	0.790578	0.6804	3.13
5	2-6	1.241159	1.0628	4.58

Table 7.12: Improvement of FIM over CPF for branch outage on IEEE 57-bus system with base loading, P_0=12.508 p.u.

No.	Branch Outage	FIM ΔP [p.u.]	CPF ΔP [p.u.]	Improvement (%)
1	35-36	-3.3589	*	-
2	25-30	0.5554	0.2977	2.01
3	34-35	1.2353	0.8555	2.84
4	37-38	2.6262	2.2564	2.50
5	1-15	5.2729	3.3283	12.30

* Convergence problem

7.6.2 Generator Outage

Results for generator outage for all the test systems with the calculated improvements are presented in Tables 7.13-7.15. Again, it can be observed that the results of FIM are better compared to CPF for all the generator outage cases, with the largest improvement recorded as 9.09% for the outage of generator 3 in IEEE 57-bus system. The improvements somehow prove the advantage of FIM in finding the security margins of a system during contingency.

Table 7.13: Improvement of FIM over CPF for generator outage for IEEE 14-bus system, P_0=2.59 p.u.

No.	Generator Outage	FIM ΔP [p.u.]	CPF ΔP [p.u.]	Improvement (%)
1	6	1.8628	1.7327	3.01
2	8	1.9804	1.7762	4.68
3	2	1.9187	1.7410	4.10
4	3	1.8712	1.7550	2.67

Table 7.14: Improvement of FIM over CPF for generator outage on IEEE 30-bus system, P_0=2.834 p.u.

No.	Generator Outage	FIM ΔP [p.u.]	CPF ΔP [p.u.]	Improvement (%)
1	8	1.3224	1.2317	2.23
2	5	1.4084	1.2730	3.30
3	2	1.4508	1.2810	4.13
4	13	1.4834	1.2813	4.91
5	11	1.5051	1.3048	4.84

Table 7.15: Improvement of FIM over CPF for generator outage on IEEE 57-bus system, P_0=12.508 p.u.

No.	Generator Outage	FIM ΔP [p.u.]	CPF ΔP [p.u.]	Improvement (%)
1	8	-1.4616	-1.4621	-
2	12	1.4476	1.2833	1.19
3	3	7.6937	6.0100	9.09
4	6	8.4062	7.1796	6.23
5	9	8.3396	7.3409	5.03
6	2	8.5136	7.3547	5.83

7.7 Discussion and Recommendations for Future Works

The hypersurface is a boundary representing a set of critical loadings. The work by Jarjis and Galiana [106] implies that the interior of the hypersurface is convex. The curve in Figure 7.12a gives a two dimensional graphical illustration of the convex hypersurface which is denoted as $\sum$. A three dimensional view of the $\sum$ is available in the work of F. Alvarado [94]. Note that each of the *x*- and *y*-axis of the curve represents a generating unit in a power system. In [107], I. Dobson agrees that the hypersurface is convex as no non-convex portions are detected in his computations. Besides, he also discusses the possibility of the hypersurface to be "corrugated", which is illustrated in Figure 7.12b.

The proposed FIM here is an advantageous approach to the present of corrugated hypersurfaces, which enable a larger security margin to be obtained. This is illustrated in Figure 7.12b whereby *A*, *B* and *C* represent the load flow solutions in the prescribed load direction. S_1 is the starting point for conventional methods and S_2 is initial point for proposed FIM method. The power margin for conventional methods will be S_1–*A* whereas by using FIM method, the obtained power margin will be S_1–*C*. Thereby, it can be observed that a larger security margin could be obtained using FIM.

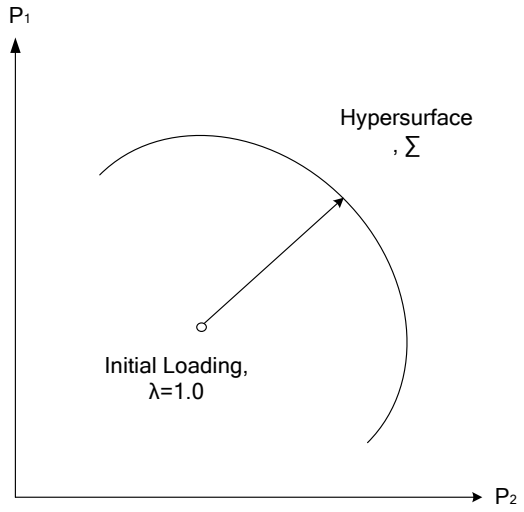

Figure 7.12a: A hypersurface curve

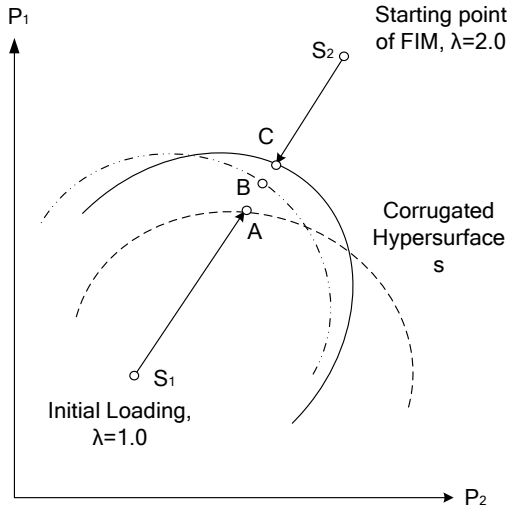

Figure 7.12b: Corrugated hypersurfaces

In future works, in order to improve the computational time of the load flow solution, other load flow approaches which can find solutions in the vicinity of critical / bifurcation point can be applied instead of using hybrid CGA/PSO as in the case of this paper. The simulation results on contingency cases can be

further extended considering multiple branch outages, multiple generator outages, or a mixture of both.

7.8 Conclusions

A method to find the Maximum Loading Point has been proposed in this paper. A mathematically proven formula has been adopted from literature to find the maximum loading margin from feasible region in the proposed Fast Infeasible Method. Determining the MLP from infeasible region is a good strategy as this is simpler and avoid complex mathematical formulation should FIM starts from feasible region. Results from the simulation on IEEE test systems have shown that better MLP values than that obtained by other methods existing in the recent literature. The branch and generator outage contingencies studies have also shown that the proposed method can find larger available security margins. This proposed FIM method is a promising approach for calculating the MLP values.

Chapter 8

8. Conclusions

In this thesis, a powerful load flow approach which is suitable for heavy-loaded systems is developed. Hereby, Particle Swarm Optimisation (PSO) algorithm is adopted as a solution acceleration method in a previous Constrained Genetic Algorithm Load Flow algorithm to further enhance the capability of that algorithm in finding a solution for large heavy-load systems. The developed algorithm in this thesis has been named as Hybrid Constrained Genetic Algorithm / Particle Swarm Optimisation, or in short form as Hybrid CGA/PSO. The experimental work in finding the optimum parameter settings for the proposed algorithm is reported in this thesis. The power of the PSO enhanced new algorithm is demonstrated through its applications to three IEEE test systems. Hybrid CGA/PSO proves to be able to find solutions on these systems with better reliability and faster speed. The maximum loading point

recorded shows improvement compared to previously found.

For application wise, the algorithm developed in this thesis is applied to locate all the Type-1 load flow solutions present in power system. In this context, Type-1 load flow solutions have been closely related to voltage stability of a system and therefore there is a demand for an efficient algorithm to locate them for voltage stability analysis. Conventional methods can only locate some of the Type-1 load flow solutions in power systems and the located solutions are inadequate for voltage stability assessment. The characteristics of the Type-1 solutions are described in the this thesis. The hybrid CGA/PSO is applied to two test systems. The test results obtained are satisfactory and promising for voltage stability monitoring applications.

Further, a stochastic method determining the maximum loading point (MLP) of electric power systems is proposed. Instead of approaching the MLP from the feasible region, a new strategy in starting from infeasible region is proposed in this thesis, which has proven to be computationally effective. Thus, this novel methodology is named as Fast Infeasible Method (FIM). The idea is simple yet interesting, and is able to obtain expected results. Underneath this algorithm is the Hybrid CGA/PSO; which has been the core method to solve the load flow problem every iteration. From the analysis, the MLP values obtained for IEEE 14-, 30- and 57-bus systems show a greater margin; which are better in comparison with existing methods. Further analysis on contingency shows

encouraging improvement in terms of available power margins when compared to CPF method. This signifies the advantage of the proposed strategy despite the random characteristic of load flow solutions in FIM.

As a conclusion, a powerful and robust algorithm for load flow approach has been developed in this thesis. This algorithm, Hybrid CGA/PSO has shown to perform effectively in locating Type-1 load flow solutions and in finding the maximum loading point of a system (MLP). The developed algorithm provides a very useful starting point for further development of tools for solving the heavy-loaded power systems containing nonlinear devices such as FACTS. This hybrid CGA/PSO is further incorporated into a proposed method (Fast Infeasible Method – FIM) in the aim of locating the MLP of a power system. Encouraging MLP values are obtained by FIM for contingencies involving generator and branch outages. Thus, hybrid CGA/PSO is a promising tool in power system and should be further developed for real world applications.

References

[1] A. M. Sasson, W. Synder, M. Flam, R. D. Masiello, B. F. Wollenberg, B. Stott, “Comments on “Review of load-flow calculation methods,” *IEEE Proc*. vol 63, no. 4, pp. 712-715, Apr. 1975.

[2] B. Stott. “Review of load-flow calculation methods,” *IEEE Proc*. vol. 62, no. 7, pp 916-929, Jul. 1974.

[3] R. D. Masiello, B. F. Wollenberg, B. Stott, “Comments on “Review of load-flow calculation methods,” *IEEE Proc*. vol 63, no. 4, pp. 713-715, Apr. 1975.

[4] W. F. Tinney and C. E. Hart, “Power flow solution by Newtons method,” *IEEE Trans. Power App. Syst.*, 86: 1449-1460, 1967.

[5] B. Stott and O. Alsac, “Fast Decoupled Load Flow,” *IEEE Trans. Power App. Syst.*, vol. PAS-93, no. 3, pp 859-869, May 1974.

[6] S. T. Despotovic, “A new decoupled load flow method,” *IEEE Trans. Power App. Syst.*, vol. PAS-93, no. 3, pp. 884-891, May 1974.

[7] M. H. Haque, “Novel decoupled load flow method,” *IEE Proc-C*, no 140, no. 3, pp 199-205, May 1993.

[8] H. Saadat: Power system analysis, McGraw-Hill, 2004.

[9] S. Iwamoto, and Y. Tamura, “A load flow calculation method for ill-conditioned power systems”, *IEEE Trans. Power App. Syst.*, vol. PAS-100, no. 4, pp. 1736-1743, Apr 1981.

[10] B. Borkowska, “Probabilistic load flow, *IEEE Trans. on PAS,* vol PAS-93, no. 3, pp. 752-759, May/Jun 1974.

[11] Chun-Lien Su, “Probabilistic load-flow computation using point of estimate method,” *IEEE Trans. Power Syst*., vol. 20, no. 4, pp. 1843-1851, Nov. 2005.

[12] Z. Hu, and Xifang Wang, “A probabilistic load flow method considering branch outages,” *IEEE Trans. Power Syst*., vol. 21, no. 2, pp. 507-514, May 2006.

[13] J. S. Throp and S. A. Naqavi, “Load flow fractals,” in *Conf. Decision Contr*., pp. 1822-1827, Dec. 1989.

[14] X. Yin, “Application of genetic algorithms to multiple load flow solution problem in electrical power systems,” in *Proc of the 32nd IEEE Conf on Decision and Control,* vol 4, pp. 3734-3738, Dec 1993.

[15] I. A. Hiskens and R. J. Davy, “Exploring the power flow solution space boundary,” *IEEE Trans. Power Syst*., vol. 16, no. 3, pp. 389-395, Aug. 2001.

[16] Y. Tamura, K. Sakamoto and Y. Tayama, “Voltage instability proximity index (VIPI) based on multiple load flow solutions in ill-conditioned

power systems", *Proc. Of 27th Conference on Decision and Control*, Austin, Texas, pp. 2114-2119, Dec 1988.

[17] Y. Tamura, H. Mori S. Iwamoto, "Relationship between voltage instability and multiple load-flow solutions in electric power systems", *IEEE Trans. Power App. Syst.*, vol. PAS-102, no.5, pp. 1115-1125, May 1983.

[18] W. Ma and J.S. Thorp, "An efficient algorithm to locate all the load flow solutions", *IEEE Trans. Power Syst*., vol. 8, no. 3, pp. 1077-1083, Aug. 1993.

[19] Songli Zhao, Hongguang Liu, Shijie Cheng, and Deshu Chen, "A new method for calculating power system multiple load flow solutions," *IEE 2nd Intl Conf on Advances in Pwr Syst Ctrl, Operation and Management*, Dec 1993, Hong Kong, pp. 274-278, Dec 1993.

[20] D. E. Goldberg. *Genetic Algorithms in Search, Optimisation and Machine Learning.* Addison-Wesley, 1989.

[21] H. Mori and F. Iizuka. "An efficient method for calculating power flow solutions and the closest bifurcation point using mathematical programming," *Proc of 1998 IEEE Intl Symp of Circuits and Sys*, vol 3, pp. 570-573, May/Jun 1998.

[22] Y. Tamura, K. Iba and S. Iwamoto, “A method for finding multiple load-flow solutions for general power systems”, *Proc. IEEE 1980 PES Winter Meeting*, A80 043-0, New York, NY, Feb. 1980.

[23] F. M. A. Salam, L. Ni., S. Guo, and X. Sun, “Parallel processing for the load flow of power systems: the approach and applications”, in *Proc. 28th Circuits Devices Conf*., Tampa, FL, pp. 2173-2178, Dec. 1989.

[24] W. Ma, and J. S. Thorp, ‘An efficient algorithm to locate all the load flow solutions’, *IEEE Trans. Power Syst*., 8, (3), pp. 1077-1083, Aug 1993.

[25] K. Iba, H. Suzuki, M. Egawa, and T. Watanabe, “A method for finding pair of multiple load flow solutions in bulk power systems”, *IEEE Trans. Power Syst*., vol. 5, no. 2, pp. 582-591, May 1990.

[26] H. D. Chiang, I. Dobson, R.J. Thomas, J.S. Thorp, and F.-A. Lazhar, “On voltage collapse in electric power systems”, *IEEE Trans. Power Syst*., vol.5, no. 2, pp. 601-611, May 1990.

[27] T. J. Overbye and R. P. Klump “Effective calculation of power system low-voltage solution”, *IEEE Trans. Power Syst.*, vol. 11, no. 1, pp. 75-82, Feb. 1996.

[28] C.-W. Liu, C.-S. Chang, J-A. Jiang, and G.-H. Yeh, “Toward a CPFLOW-based Algorithm to Compute All the Type-1 Load Flow Solutions in Electric Power Systems”, *IEEE Trans. Circuits Syst.*, vol. 52, no. 3, pp. 625-629, March 2005.

[29] C.L. DeMarco and A. R. Bergen, “A security measure for random load disturbances in nonlinear power system models,” *IEEE Trans. Circuits and Systems*, vol. CAS-34, no. 12, pp. 1546-1557, Dec. 1987.

[30] T. J. Overbye, C. L. Demarco, "Improved Technique for Power System Voltage Stability Assessment Using Energy Methods", *IEEE Trans. Power Syst.*, Vol. 6, No. 4, pp. 1496-1452, Nov 1991.

[31] L. A. L. Zarete, and C. A. Carlos, J. M. Ramos, and E. R. Ramos: ‘Fast computation of voltage stability security margins using nonlinear programming techniques’, *IEEE Trans. Power Syst*., 21, (1), pp. 19-27, Feb 2006.

[32] L. A. L. Zarete, and C. A. Carlos: ‘Fast computation of security margins to voltage collapse based on sensitivity analysis,’ *IEE Proc. Gener. Transm. Distrib*., 153, (1), pp. 19-26, Jan 2006.

[33] P.-A. Lof, G. Andersson, and D. J. Hill, “Voltage stability indices for stressed power systems”, *IEEE Trans. Power Syst*., vol. 8, no. 1, pp. 326-335, Feb 1993.

[34] C. Cãnizares, A. C. Z. Souza, and V. Quintana, ‘Comparison of performance indices for detection of proximity to voltage collapse’, *IEEE Trans. Power Syst*., 11, (3), pp. 1441-1450, Aug 1996

[35] Z. C. Zeng, F. D. Galiana, B. T. Ooi, and N. Yorino, "A simplified approach to estimate maximum loading conditions", *IEEE Trans. Power Syst.*, vol 8, no. 2, pp. 645-654, May 1993.

[36] V. Ajjarapu and C. Christy, "The continuation power flow: A tool for steady state voltage stability analysis," *IEEE Trans. Power Syst.*, vol. 7, no. 1, pp. 416-423, Feb. 1992.

[37] W. F. Tinney, and C. E. Hart, 'Power flow solution by Newton's method', *IEEE Trans. Power App. Syst*., PAS-86, pp.1449-1460, Nov 1967

[38] L. M. C. Braz, C. A. Castro, and C. A. F. Murari, 'A critical evaluation of step size optimization based load flow methods', *IEEE Trans. Power Syst*., 15, (1), pp. 202-207, Feb 2000

[39] F. D. Galiana, and Z. C. Zeng, "Analysis of the load flow behavior near a Jacobian singularity", *IEEE Trans. Power Syst*., vol. 7, no. 3, pp. 1362-1369, Aug 1992.

[40] G. D. Irissari, X. Wang, and S. Mokthari, "Maximum loadability of power system using interior point non-linear optimization method", *IEEE Trans. Power Syst*., vol. 12, no. 1, pp. 162-172, Feb 1997.

[41] G. L. Torres, V. H. Quintana, and M. A. Carvalho, "Higher-order interior point methods for computing minimum load shedding and maximum loadability of power systems". *8th Symp. On Specialists in Electric*

Operational and Expansion Planning (8th SEPOPE), Brasilia, Brazil, May 2002.

[42] N. Flatabo, R. Ognedal, and T. Carlsen, "Voltage stability condition in a power transmission system calculated by sensitivity methods," *IEEE Trans. Power Syst.*, vol. 5, no. 4, pp. 1286-1293, Nov. 1990.

[43] N. Flatabo, O. Fosso, R. Ognedal, and T. Carlsen, "A method for calculation of margins to voltage instability applied on the Norwegian system for maintaining required security level," *IEEE Trans. Power Syst*. vol. 9, no. 2, pp. 906-917, May 1994.

[44] A. C. Z. Souza, L. M. Honorio, G. L. Torres, and G. Lambert-Torres, "Increasing the loadability of power system through optimal-local control actions," *IEEE Trans. Power Syst*., vol. 19, no. 1, pp. 188-194, Feb. 2004.

[45] Y. Mansour, Ed., Suggested Techniques for Voltage Stability Analysis. Piscataway, NJ: IEEE Press, 1993. 93TH0620-5PWR.

[46] I. Dobson, "Computing an optimal direction in control space to avoid saddle node bifurcation and voltage collapse," *IEEE Trans. Automat. Contr.*, vol. 37, pp. 1616-1620, Oct. 1992.

[47] S. Greene, I. Dobson, and F.L. Alvarado, "Sensitivity of the loading margin to voltage collapse with respect to arbitrary parameters," *IEEE Trans. Power Syst.*, vol. 12, pp. 262-272, Feb. 1997.

[48] N. Yorino, S. Harada, K. Hayashi, and H. Sasaki, “A method of voltage stability evaluation for contingencies,” presented at the *Bulk Power System Dynamics and Control IV*, Santorino, Greece, Aug. 1998.

[49] S. Greene, I. Dobson, and F. L. Alvarado, “Contingency ranking for voltage collapse via sensitivity from a single nose curve,” *IEEE Trans. Power Syst*., vol. 15, pp. 232-240, Feb. 1999.

[50] H. D. Chiang, C. S. Wang, and A. J. Flueck, “Look-ahead voltage and load margin contingency selection functions for large-scale power system,” *IEEE Trans. Power Syst.*, vol. 14, pp. 327-335, Feb. 1999.

[51] F. Capitanescy and T. Van Cutsem, “Evaluation of reactive power reserves with respect to contingencies,” presented at the *Bulk Power System Dynamics and Control V*, Onomichi, Japan, Aug. 26-31, 2001.

[52] H. Liu, A. Bose, and V. Venkatasubramanian, “A fast voltage security assessment method using adaptive bounding,” *IEEE Trans. Power Syst.*, vol. 15, pp. 1137-1141, Aug. 2000.

[53] N. Yorino, H.Q. Li, S. Harada, A. Ohta and H. Sasaki, “A method of voltage stability evaluation for branch and generator outage contingencies,” *IEEE Trans. Power Syst.*, vol. 19, pp. 252-259, Feb. 2004.

[54] K. P. Wong, A. Li and M.Y. Law, “Development of constrained-genetic-algorithm load-flow method”, *IEE Proc. Gener. Transm. Distrib*., vol. 144, no. 2, pp. 91-99, Mac 1997.

[55] K.P. Wong, A. Li and T.M.Y. Law, "Advanced constrained genetic algorithm load flow method", *IEE Proc. Gener. Transm. Distrib.*, vol. 146, no. 6, pp. 609-616, Nov 1999.

[56] D. E. Goldberg. Genetic Algorithms in Search, Optimization, and Machine Learning. Addison Wesley, Reading (MA), 1989.

[57] J. H. Holland. Adaptation in Natural and Artificial Systems. MIT Press, Cambridge (MA), 2nd edition, 1992.

[58] Z. Michalewicz. Genetic Algorithms + Data Structures = Evolution Programs. Springer, Berlin and Heidelberg, 3rd edition, 1996.

[59] T. Back and H.-P. Schwefel, "An overview of evolutionary algorithms for parameter optimization," *Evolutionary Computation*, vol. 1, no. 1, pp. 1-23, 1993.

[60] L. J. Fogel, A. J. Owens, and M. J. Walsh, *Artificial Intelligence Through Simulated Evolution*, John Wiley & Sons, New York, NY, 1966.

[61] J. Kennedy, and R. C. Eberhart, 'Particle swarm optimization', in *Proc. IEEE Int. Conf. Neural Netw.*, pp. 1942-1948, Nov/Dec 1995.

[62] Y. Shi., and R. C. Eberhart, 'A modified particle swarm optimizer', in *Proc. IEEE Int. Conf. Evol. Comput.*, Anchorage, Alaska, 1998. pp. 69-73

[63] F. Li, R. Morgan and D. Williams, "Hybrid genetic approaches to ramping rate constrained dynamic economic dispatch, *Electric Power Systems Research*, 43(11), pp. 97-103, 1997.

[64] C. C. Lo and W. H. Chang, "A multiobjective hybrid genetic algorithm for the capacitated multipoint network design problem," *IEEE Trans. Sys, Man and Cybernetics – B*, vol. 30, no. 3, pp. 461-470, Jun 2000.

[65] P. Somasundaram, R. Lakshmiramanan, and K. Kuppusamy, "Hybrid algorithm based on EP and LP for security constrained economic dispatch problem, *Electric Power Systems Research*, vol 76 (1-3), pp. 77-85, 2005.

[66] G. Magyar, M. Johnsson, and O Nevalainen, "An adaptive hybrid genetic algorithm for the three-matching problem," *IEEE Trans. on Evol Comp*, vol. 4, no. 2, pp. 135-146, Jul 2000.

[67] A. Sinha and D. E. Goldberg, "A survey of hybrid genetic and evolutionary algorithms," *ILLIGAL Technical Report 2003004*, 2003.

[68] D. H. Wolpert and W. G. Macready, "No free lunch theorems for optimization, *IEEE Trans. Evol Comp.* Vol 1, No. 1, pp. 67-82, Apr 1997.

[69] A. K. Swain and A. S. Morris, "A novel hybrid evolutionary programming method for function optimization," In *Proc of the Congress on Evolutionary Computation (CED200)*, pp. 1369-1376, 2000.

[70] W. E. Hart, N. Krasnogor, and J. E. Smith, "Recent advances in memetic algorithms, Series: *Studies in Fuzziness and Soft Computing*, vol. 166, 2005.

[71] P. Moscato, "Memetic algorithms: A short introduction, in new ideas in optimization, Corne et al. D (Eds.), pp. 219-234, 1996.

[72] M. Clerc and J. Kennedy, “The particle swarm: explosion stability and convergence in a multi-dimensional complex space,” *IEEE Trans on Evol Comp*., Vol 6, No 1, pp. 23-33, Feb 2002.

[73] R. C. Eberhart and J. Kennedy, “A new optimizer using particle swarm theory,” In *Proc of 6th Intl Symp. On Micro Machine and Human Science*, Nagoya, Japan, IEEE Service Center, Piscataway, NJ, pp. 39-43, Oct 1995.

[74] J. Kennedy and R. C. Eberhart, “Particle swarm optimization,” In *Proc of IEEE Intl Conf on Neural Networks*, Perth, Australia, pp. 1942-1948, 1995.

[75] D. H. Kim and J. H. Cho, “Robust tuning of PID controller using bacterial-foraging-based optimization,” *JACIII* 9(6), pp. 669-676, 2005.

[76] X. H. Shi, Y. C. Liang, H. P. Lee, C. Lu, and L.M. Wang, “An improved GA and a novel PSO-GA-based hybrid algorithm,” *Information Processing Letters*, Vol 93, No. 5, pp. 255-261, 2005

[77] E. A. Grimaldi, F. Grimacia, M. Mussetta, P. Pirinoli, and R. E. Zich, “A new hybrid genetic-swarm algorithm for electromagnetic optimization, In *Proc of Intl Conf on Comp Electromagnetics and its Applications*, Beijing, China, pp. 157-160, 2004.

[78] C. Grosan, A. Abraham, and M. Nicoara, “ Search optimization using hybrid particle sub-swarms and evolutionary algorithms, *Intl Journal of*

Simulation Systems, Science and Technology, UK, vol 6 (10-11), pp. 60-79, 2005.

[79] H. Liu, A. Abraham, and W. Zhang, "A fuzzy adaptive turbulent particle swarm optimization, *Intl Journal of Innovative Computing and Applications*, vol 1, no. 1, pp. 29-47, 2007.

[80] C. Grosan, A. Abraham, and M. Nicoara, "Search optimization using hybrid particle sub-swarms and evolutionary algorithms, *Intl Journal on Simulation Systems, Science and Technology*, UK, vol. 6 (10-11), pp. 60-79, 2005.

[81] B. Zhao, C. X. Guo, and Y. J. Cao, 'A multiagent-based particle swarm optimization approach for optimal reactive power dispatch', *IEEE Trans. Power Syst.*, 20, (2), pp. 1070-1078, 2005.

[82] J.-B. Park, K.-S. Lee, J.-R. Shin, and K. Y. Lee 'A particle swarm optimization for economic dispatch with non-smooth cost functions', *IEEE Trans. Power Syst.*, 20, (1), pp. 34-42, Feb 2005

[83] M. A. Abido, 'Optimal design of power-system stabilizers using particle swarm optimization', *IEEE Trans. Energ. Conv.*, 17, (3), pp. 406-413, Sept 2002.

[84] M. Clerc, and J. Kennedy, 'The particle swarm: Explosion, stability, and convergence in a multi-dimensional complex space', *IEEE Trans. Evol. Comput*., 6, (1), pp. 58-73, 2002

[85] A. Chatterjee, K. Pulasinghe, K. Watanabe, and K. Izumi.: 'A particle-swarm-optimized fuzzy-neural network for voice-controlled robot systems', *IEEE Trans. on Industrial Electronics.*, 52, (6), pp. 1478-1489, Dec 2005.

[86] N. D. Hatziargyriou, and T. S. Karakatsanis, "Probabilistic constrained load flow for optimizing generator reactive power resources," *IEEE Trans. Power Syst*., vol. 15, no. 2, pp. 687-693, May 2000.

[87] C. W. Taylor, "Power System Voltage Stability", McGraw-Hill, New York, 1994.

[88] P. Kundur, "Power System Stability and Control", McGraw-Hill, New York, 1994.

[89] A. Dimitrovski, K. Tomsovic, "Boundary load flow solutions", *IEEE Trans. Power Syst*., vol. 19, no. 1, pp. 348-355, Feb. 2004.

[90] T. J. Overbye, "Effects of load modelling on analysis of power system voltage stability," *Int. J. Elect. Power Energy Syst*., vol. 16, no. 5, pp. 329-339, 1994.

[91] C.-W. Liu and J. S. Thorp, "A novel method to compute the closest unstable equilibrium point for transient stability region estimate in power system", I*EEE Trans. Circuits Syst. I: Fundam. Theory Applicat.*, vol. 44, no. 7, pp. 630-635, Jul. 1997.

[92] T. O. Ting, K. P. Wong and C. Y. Chung, "A Hybrid Genetic Algorithm/Particle Swarm Approach for Evaluation of Power Flow in Electric Network" *Lecture Notes in Computer Science*, vol 3930, pp. 908-917, May 2006.

[93] J. Lu, C.W. Liu, and J.S. Thorp, "New methods for computing a saddle node bifurcation point for voltage stability analysis," *IEEE Trans. Power Syst*., vol 10, no. 2, pp. 978-989, May 1995.

[94] F.L. Alvarado, I. Dobson, R.J. Thomas, and Y. Hu, "Computation of closest bifurcation in power systems," *IEEE Trans. Power Syst*., vol. 9, no. 2, pp. 918-928, May 1994.

[95] I. Dobson, "Observations on the geometry of saddle node bifurcations and voltage collapse in electrical power systems", *IEEE Trans. Circuits and Syst.-I*, vol. 39, no. 3, pp. 240-243, Mar 1992.

[96] K. Chen, A. Hussien, M. E. Bradley, and H. Wan, "A performance-index guided continuation method for fast computation of saddle-node bifurcation in power systems," *IEEE Trans. Power Syst.*, vol 18, no. 2, pp. 753-760, May 2003.

[97] H. D. Chiang, "Application of Bifurcation Analysis to Power Systems," Bifurcation Control, LNCIS 293, pp. 1-28, 2003.

[98] A. J. Flueck, R. Gonella, and J. R. Dondeti, “A new power sensitivity method of ranking branch outage contingencies for voltage collapse,” *IEEE Trans. Power Syst*., vol. 17, no. 2, pp. 265-270, May 2002.

[99] T.O. Ting, K.P. Wong, C.Y. Chung, “Locating Type-1 Load Flow Solutions using Hybrid Evolutionary Algorithm” *Proc. of the 5th IEEE Intl Conf on Machine Learning and Cybernetics (ICMLC 2006)*, Dalian, China, vol 7, pp. 4093-4098, Aug 2006..

[100] National System Operator (ONS). Network Procedures: Guidelines and Criteria for Electrical Studies, Submodule 23.3 (in Portuguese). [Online]. Available: http://www.ons.org.br/ons/procedimentos/index.html.

[101] N. Yorino, S. Harada, and H. Cheng, “A method to approximate a closest loadability limit using multiple load flow solutions,” *IEEE Trans. Power Syst.*, vol 12, no. 1, pp. 424-429, Feb 1997.

[102] F. Milano, A. J. Conejo, and R. Zárate-Minano, “General sensitivity formulas for maximum loading conditions in power systems,” *IET Gener. Transm. Distrib*., vol 1, no. 3 , pp. 516-526, May 2007.

[103] A. Sode-Yome, N. Mithulananthan, and K. Y. Lee, “A maximum loading margin method for static voltage stability in power systems,” *IEEE Trans. Power Syst.*, vol 21, no. 2, pp 799-808, May 2006.

[104] Power Systems Test Case Archive, University of Washington College of Engineering. [Online]. Available: http://www.ee.washington.edu/research/pstca/ , accessed on May 2006.

[105] F. Milano. (2002) PSAT, Matlab-Based Power System Analysis Toolbox. [Online] Available at: http://thunderbox.uwaterloo.ca/~fmilano

[106] J. Jarjis, and F. D. Galiana, "Quantitative analysis of steady state stability in power networks," *IEEE Trans. Power App. Syst*., vol 100, no. 1, Jan 1981.

[107] I. Dobson,, and L. Lu, "New methods for computing a closest saddle node bifurcation and worst case load power margin for voltage collapse," *IEEE Trans. Power Syst*., vol 8, no. 3, pp. 905-913, Aug. 1993.